AGU ADVANCING EARTH AND SPACE SCIENCES

Water Resources Research

RESEARCH ARTICLE
10.1029/2025WR041436

Assessing the Effectiveness of Nature-Based Solutions and Building-Level Flood Risk Reduction Measures: An Open-Source Coupled Model

Veerle C. Bril[1], Jens de Bruijn[1,2], Hans de Moel[1], Tarun Sadana[1], Tim Busker[1], W. J. Wouter Botzen[1], and Jeroen C. J. H. Aerts[1,3]

[1]Institute for Environmental Studies (IVM), Vrije Universiteit Amsterdam, Amsterdam, The Netherlands, [2]International Institute for Applied Systems Analysis (IIASA), Laxenburg, Austria, [3]Deltares, Delft, The Netherlands

Key Points:

- We extend the socio-hydrological Geographical, Environmental, and Behavioral model with a hydrodynamic, flood risk and adaptation model
- Both nature-based solutions (NBS) (−38%) and building-level adaptation measures (−95%) perform well in reducing flood risk
- Benefit-cost ratios are highest for dry-proofing (1.23) and wet-proofing (1.14), while NBS are more difficult to monetize

Supporting Information:

Supporting Information may be found in the online version of this article.

Correspondence to:

V. C. Bril,
v.c.bril@vu.nl

Citation:

Bril, V. C., de Bruijn, J., de Moel, H., Sadana, T., Busker, T., Botzen, W. J. W., & Aerts, J. C. J. H. (2026). Assessing the effectiveness of nature-based solutions and building-level flood risk reduction measures: An open-source coupled Model. *Water Resources Research*, *62*, e2025WR041436. https://doi.org/10.1029/2025WR041436

Received 23 JUN 2025
Accepted 18 FEB 2026

Author Contributions:

Conceptualization: Veerle C. Bril, Jens de Bruijn, Hans de Moel, Tim Busker, W. J. Wouter Botzen, Jeroen C. J. H. Aerts
Formal analysis: Veerle C. Bril
Funding acquisition: Jeroen C. J. H. Aerts
Methodology: Veerle C. Bril, Jens de Bruijn, Hans de Moel, Tarun Sadana, Tim Busker, W. J. Wouter Botzen, Jeroen C. J. H. Aerts
Project administration: Jeroen C. J. H. Aerts
Resources: Jeroen C. J. H. Aerts
Software: Veerle C. Bril, Jens de Bruijn, Tarun Sadana, Tim Busker

Abstract Floods are expected to increase in frequency and severity due to climate change. Recent floods have shown that many catchments worldwide are vulnerable to floods, highlighting the need for additional adaptation measures. This study extends the Geographical, Environmental, and Behavioral (GEB) model by coupling it to a hydrodynamic and a flood risk model to assess the effects of dry-proofing, wet-proofing, retention ponds, reforestation, and the creation of natural grassland. A key innovation is the integration of all local-scale models, thereby allowing for a catchment-wide assessment of the impacts of various measures on interlinked hydrological conditions, flood extents and depths, damages, and risk. We apply our method to the Geul catchment (shared between the Netherlands, Belgium and Germany), which was heavily flooded in July 2021. Our results show that reforestation and creation of natural grassland (both 10 km^2) reduce flood extent by 12% and average water depth by 10%. Damage is decreased up to 38%. Larger retention ponds (1 m deeper) have a much smaller reduction in flood extent (3%), depth (0.5%) and damage (1.6%), due to limited storage capacity compared to excess rainfall. The building-level adaptation scenarios outperform all nature-based solutions, with dry-proofing reducing more damage (up to 95%) than wet-proofing (around 55%). A cost-benefit analysis shows that several adaptation measures are economically attractive. Overall, our findings show a coupled model is essential for comparing the relative effectiveness of different flood adaptation measures and supporting informed risk management decisions. The open-source model is transferable to other catchments worldwide to guide decision-making.

Plain Language Summary Floods are expected to increase in frequency and severity due to climate change, threatening people worldwide. To limit future damage, additional adaptation measures are needed. Understanding how well these measures work requires reliable models. However, different measures often require different types of models, which makes it difficult to compare their effectiveness. Therefore, in this study, we further develop the Geographical, Environmental, and Behavioral (GEB) model so that several adaptation measures can be assessed within a single framework. We simulate the effects of nature-based solutions (retention ponds, reforestation, creating natural grasslands) and building-level adaptation measures (dry-proofing, wet-proofing). The model is applied to the Geul catchment, which experienced severe flooding in July 2021. Our results show that creating larger retention ponds has only limited effectiveness, reducing damage by only 1.6%. Reforestation and creating natural grassland result in a damage reduction of 38%. The most effective measures are the building-level adaptation measures, which reduce damage by 55% (wet-proofing) and 95% (dry-proofing). The improved GEB model can also be used in other regions to assess how effective these measures might be elsewhere.

1. Introduction

Flooding causes large damages: in the period 2018–2022 global flood losses amounted to $300 billion (Munich RE, 2023). It is expected that the frequency and severity of floods will increase because of climate change (Arnell & Gosling, 2016). One of the recent, large flood events was the July 2021 flood that hit parts of Northwestern Europe, severely impacting Germany, Belgium, and the Netherlands, leading to over 200 casualties (Mohr et al., 2023). In the Netherlands, no fatalities occurred, but direct damages were in the hundreds of millions (Jonkman et al., 2023). One of the worst hit places was the city of Valkenburg along the Geul river, a trans-boundary tributary of the Meuse river. The Netherlands has the highest flood safety standards in the world (Chan et al., 2022), which has been achieved primarily by building levees. However, these high safety standards are only

Supervision: Jens de Bruijn, Hans de Moel, Tim Busker, W. J. Wouter Botzen, Jeroen C. J. H. Aerts
Validation: Veerle C. Bril
Visualization: Veerle C. Bril
Writing – original draft: Veerle C. Bril
Writing – review & editing: Veerle C. Bril, Jens de Bruijn, Hans de Moel, Tarun Sadana, Tim Busker, W. J. Wouter Botzen, Jeroen C. J. H. Aerts

applicable to the coast and major rivers (Meuse and Rhine rivers) and not to small tributaries such as the Geul, which has an average discharge of only ~4 m^3/s (Tsiokanos et al., 2024). In this setting, high levees are not feasible because of the lack of space, high costs, or factors that may influence the aesthetic character of the area (e.g., Aerts, 2018).

Therefore, smaller-scale measures need to be considered in addition to flood protection works. Households can, for example, reduce their flood risk by implementing wet- or dry-proofing measures (Endendijk et al., 2023a). With wet-proofing measures, water can still enter the home, but damage is minimized. For example, flood losses can be reduced by placing electrical installations at higher locations or by changing a wooden floor into a more water-resistant tile floor. Dry-proofing measures, e.g., by installing a flood shield at the front of a house, aim to prevent floodwater from entering (e.g., Aerts & Botzen, 2011). These relatively inexpensive building-level measures can reduce flood damage by up to 40% (Endendijk et al., 2023a).

However, not all damage can be prevented with building-level measures. Therefore, the government in the Geul area is assessing the added value of nature-based solutions (NBSs) in upstream rural areas (Otto et al., 2016; Santoro et al., 2019). These measures aim to create or restore ecosystems while reducing flood risk. Upstream NBS measures include reforestation and wetland restoration to enhance evaporation and storage (Gutman, 2019; Nadal-Romero et al., 2023). Downstream NBSs include enhancing the natural flow of rivers by reintroducing meandering to slow down discharge (Della Justina et al., 2019). Several studies have analyzed the effects of NBSs on flood peaks, flood extent, and flood risk (e.g., Agarwal et al., 2024; Ferreira et al., 2020; Guido et al., 2023; Ruangpan et al., 2020). While these studies show the potential of NBSs to reduce flood hazard and risk at the local scale, Ruangpan et al. (2020) state that there is a research gap in assessing the effects of NBSs at a catchment scale. Furthermore, only a few studies (e.g., Lallemant et al., 2021; Pudar et al., 2020; Ruangpan et al., 2024) have valued the flood risk reduction of NBSs in monetary terms through a modeling approach. For example, Lallemant et al. (2021), in a case study in Myanmar, found that reforestation can reduce flood risk by $1 million/year by 2040, corresponding to a 14% decrease in expected annual damage (EAD). Pudar et al. (2020) calculated that detention ponds can reduce flood risk by €3.45 million/year (86% decrease in EAD) in Serbia. Ruangpan et al. (2024) investigated the effects of several NBSs in Serbia. They found a flood risk reduction of €0.488 million/year for reforestation (11% decrease in EAD), €1.394 million/year for retention ponds (32% decrease in EAD) and €0.0097 million/year for floodplain restoration (2% decrease in EAD).

The existing studies on the performance of NBSs for reducing flood risk seem promising. Yet, in practice, the uptake of NBSs remains limited because knowledge is lacking on their (monetary) benefits, especially at a catchment level, including their relative contribution compared to other types of measures (Martin et al., 2025; Opperman & Galloway, 2022). For example, most NBS-studies evaluate only one local NBS measure (e.g., Lallemant et al., 2021; Pudar et al., 2020), while several of these measures can be implemented simultaneously in a river catchment. Furthermore, to make informed decisions, it is necessary to compare the effectiveness of different NBSs to other types of measures (large- and local-scale flood protection) and test combinations of various measures under different flooding scenarios (Kumar et al., 2021). However, in the current literature, NBSs are only compared to large-scale flood protection measures such as dikes (e.g., Pudar et al., 2020; Turkelboom et al., 2021; Vojinovic et al., 2021).

Despite the promising first studies on the effectiveness of NBSs and building-level measures for flood risk reduction, to our knowledge, no studies have holistically evaluated the benefits of these different type of measures on a catchment scale. Most studies either use a setup where they use combinations of hydrological and hydrodynamic models, which sometimes are manually coupled (e.g., Ferreira et al., 2020), or couple their set up to a damage model (e.g., Lallemant et al., 2021; Vojinovic et al., 2021). However, to date, many models have lacked an automatic setup that can evaluate the effectiveness of several types of adaptation measures, such as NBSs, building-level measures, or technical measures, which have interlinked effects on hydrological conditions, flood extents and depths, damages and flood risk. Moreover, a holistic evaluation (e.g., through cost-benefit analysis, CBA) has been done for NBSs (e.g., Ruangpan et al., 2024) and for combinations of gray and green measures (e.g., Le Coent et al., 2021) but has not yet been implemented in a comparison of NBSs and building-level measures.

Given these research gaps, the aim of this paper is to assess the risk reduction of building-level adaptation measures and three NBSs (retention ponds, reforestation, and the creation of natural grassland instead of cropland). All measures are modeled in a way that reflects their maximum possible effect. The Geul catchment in the

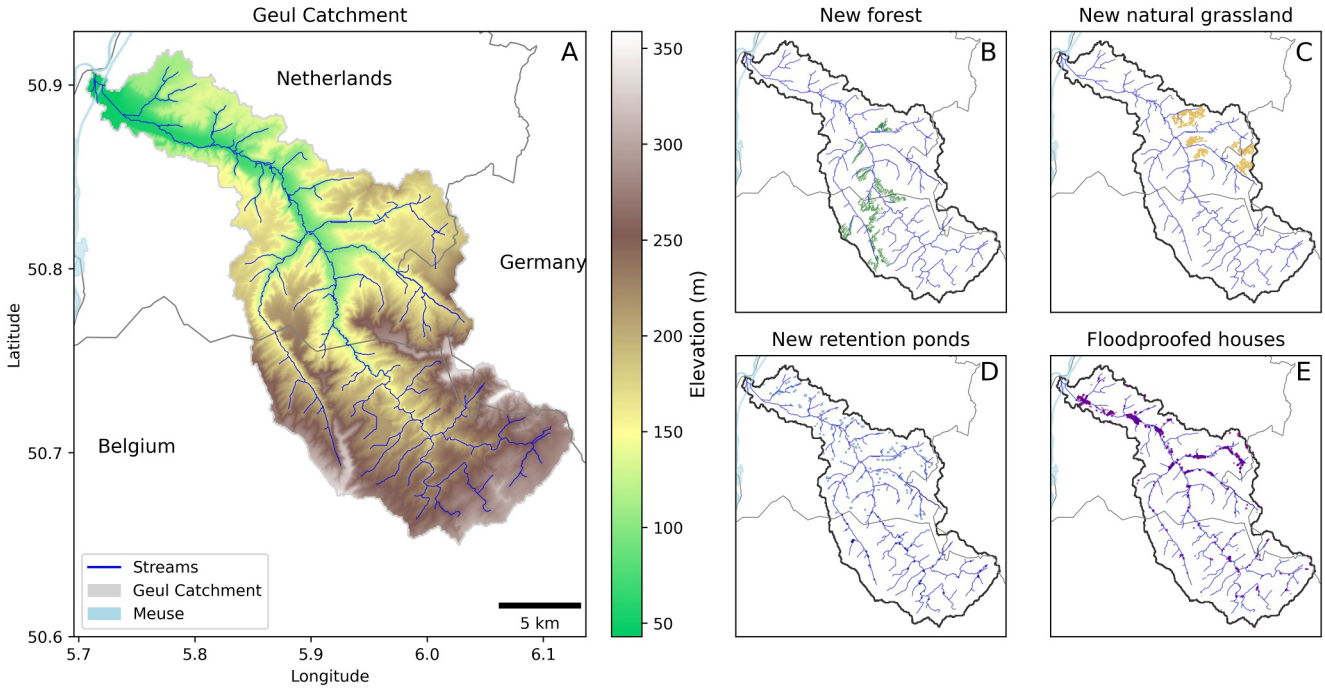

Figure 1. (a) Location of the Geul River catchment area, together with the stream network and the elevation, (b) Locations of reforestation scenario (see 3.4), (c) Locations of cropland that is converted into natural grassland (see 3.4), (d) Locations of the existing retention ponds in lighter blue and newly created ponds in dark blue, and (e) All houses located in the 1 in 1,000 years floodzone which are used for the dry- and wet-proofing scenarios (see 3.5).

Netherlands is used as an exemplar of small, flood-prone river basins in temperate Europe, where additional adaptation measures are needed to reduce flood risk. This case is particularly relevant because the regional Water Board (a governmental organization responsible for water management) is currently developing NBSs such as retention ponds and considering more widespread adoption of building-level adaptation measures. The results of this study therefore provide both scientific insights and practical guidance for the implementation of such measures in similar international contexts.

To achieve this aim, the study has the following objectives: (a) to extend the open-source socio-hydrological model GEB (Geographical, Environmental and Behavioral model; De Bruijn et al., 2023) with the hydrodynamic model SFINCS and an object-based flood risk model; (b) to use detailed building-level exposure and vulnerability data in the flood risk model, with data specifically collected for our case study area; (c) to perform CBA of all measures. This approach allows for a detailed, object-based assessment of flood risk reduction strategies and their implications for flood risk management in small, flood-prone catchments.

The remainder of the paper is structured as follows: Section 2 describes the Geul case study area, after which we explain our methodology (Section 3) and present the main results (Section 4). We discuss these results in Section 5, after which we provide our main conclusions in Section 6.

2. Case Study Description

The Geul River is a tributary of the Meuse and is located in the Netherlands, Belgium, and Germany (Figure 1). The total catchment area is approximately 340 km^2 (Van Heeringen et al., 2022). The Geul River flows through a hilly catchment with elevation ranging from 50 to approximately 340 m over a distance of 58 km (Van Heeringen et al., 2022). The yearly average precipitation is ~870 mm/year with only slightly more rainfall in the winter period (Tsiokanos et al., 2024). The land use can be roughly divided into three zones: agriculture on the plateaus, forest on the steep hills and grassland in the river valleys (Van Heeringen et al., 2022). During heavy rainfall events, the water flows quickly from the hills into the streams, resulting in local flash floods and damage to buildings. For the Dutch part of the catchment, the regional flood protection standard is 1 in 25 years, and the

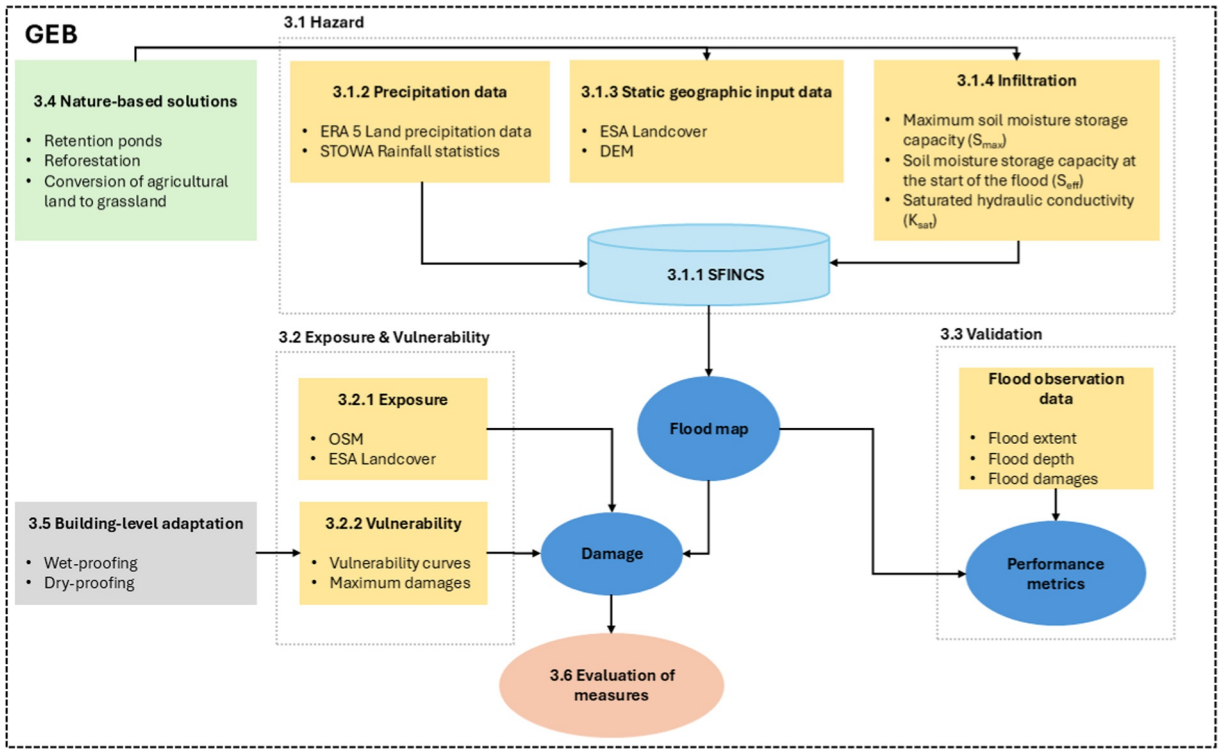

Figure 2. Framework depicting the modeling steps taken in the analysis. GEB = Geographical, Environmental, and Behavioral model; ERA = ECMWF Re-Analysis, STOWA = Stichting Toegepast Onderzoek Waterbeheer (translation: Foundation for Applied Research in Water Management), ESA = European Space Agency, SFINCS = hydrodynamic model (Super-Fast INundation of CoastS); DEM = Digital Elevation Model; OSM = OpenStreetMap. Numbers indicate the sections in which each step is described.

development and maintenance of flood protection measures is the responsibility of the local water authority, which is the Water Board Limburg (ENW - Task Force Fact Finding Hoogwater, 2021).

In July 2021, Germany, Belgium, and the Netherlands were struck by heavy rainfall and severe floods. In the Netherlands, 150–200 mm was recorded in 28 hr in the area surrounding the Geul catchment, which resulted in large-scale flooding (Mohr et al., 2023; Tsiokanos et al., 2024). The Geul River also flooded, reaching estimated peak discharges of 100 m^3/s (ENW - Task Force Fact Finding Hoogwater, 2021). The total damage in the region is estimated at approximately €250 million (ENW - Task Force Fact Finding Hoogwater, 2021; Kok et al., 2023). Following this event, a discussion was initiated to develop new flood adaptation measures for the area (Jonkman et al., 2023).

3. Methodology

Figure 2 presents a framework to evaluate the performance of several NBSs and building-level adaptation measures, the components of which are described in detail in the sections below. The yellow boxes represent input data sets: precipitation data (3.1.2), static geographic input data describing the catchment (3.1.3), and infiltration data (3.1.4). The circles represent model outputs. The input data is used in the hydrodynamic model SFINCS (3.1.1) to generate flood extent maps for several return periods based on rainfall statistics. In Section 3.2, the exposure (3.2.1) and vulnerability (3.2.2) data are described, which are used to calculate damage for each flood event. In Section 3.3, the simulations are compared to observed flood hazard data to validate the model. In the baseline model, two types of measures are introduced: NBSs (3.4) and building-level adaptation measures (3.5). In Section 3.6, the performance of the measures is evaluated using flood extent, average flood depth, damages, and costs. The damages and costs are combined into a cost-benefit analysis (CBA).

The framework is implemented in the existing GEB model (de Bruijn et al., 2023; Kalthof et al., 2025). GEB has been used before to simulate the adaptation decisions of farmers under drought conditions (de Bruijn et al., 2023; Kalthof et al., 2025). The model previously consisted of a hydrological module and an agent-based model (i.e., a

model designed to capture the behavior of autonomous individuals farmers, Kalthof et al., 2025), but non-farming households were not included individually. In this paper we expand the model by integrating the hydrodynamic model SFINCS (Section 3.1.1) and by creating a new flood risk module (Section 3.2). We also (for the first time) include individual non-farming households and their homes, but in this paper have not yet implemented autonomous dynamic behavior for household agents. This is, however, ongoing work and will be included in a future version. Thus, in this manuscript, we do not use autonomous decisions to simulate adaptation decisions, instead our objective is to assess the maximum potential flood risk reduction achievable by a set of adaptation measures, both by individuals and governments.

3.1. Hazard

3.1.1. SFINCS Model

SFINCS is a 2D hydrodynamic model with reduced complexity, allowing for rapid simulations (Leijnse et al., 2021). It uses the simplified Saint-Venant equations of mass and momentum and subgrid discretization (Leijnse et al., 2021). SFINCS has been successfully used to simulate compound flooding (Leijnse et al., 2021) and coastal flood hazard (Parodi et al., 2020; Röbke et al., 2021), as well as studies to assess flood damages (e.g., Sebastian et al., 2021). SFINCS can be set up with different types of forcing data, such as storm surge, precipitation rates, or upstream discharge. In this study, we use SFINCS to set up a flood model where precipitation is used as the primary forcing, because there is no inflow from other rivers within the Geul catchment. We chose to use SFINCS in this study because of the short computation time, which makes it possible to compare a wide range of alternative adaptation scenarios and rainfall events. We run SFINCS at a spatial resolution of 5 m with a grid of 60 m and a subgrid of 12 cells per gridcell. We did not calibrate the model.

3.1.2. Precipitation Data

We create design rainfall events for each return period using national extreme value rainfall statistics from STOWA (see Table S1 in Supporting Information S1; Nicolai et al., 2024). We assume that the total accumulated rainfall falls evenly in time and space; therefore, each pixel receives the same amount of rainfall every hour. We use return periods ranging from 25 to 1,000 years, since floods with smaller return periods are assumed to be fully protected against, given that the protection standard in the catchment is 1 in 25 years. For validation of our model, we also add the actual 2021 flood event, thus allowing comparison with observations. Precipitation data from the ERA5-Land data set is used for the period 02-07-2021 until 16-07-2021 covering the 2021 flood event, including several days before and after the event (Muñoz Sabater, 2019). Averaged over the catchment, the ERA5-Land rainfall during this event was 97 mm over 48 hr (during July 14th and 15th), corresponding to a return period of 1 in 50 years.

3.1.3. Static Geographic Input Data

Land use data: Land use patterns are derived from the ESA WorldCover 2021 data at 10 m spatial resolution (Zanaga et al., 2022). In addition, to parametrize the SFINCS model with Manning's roughness, we use the relation between land use types and Manning's roughness (Table S2 in Supporting Information S1) estimated by Deltares (2024a).

River network: We use a Digital Elevation Model (DEM) with a resolution of 5 m developed by De Jong and Asselman (2022), who merged elevation data sets from the Netherlands, Belgium, and Germany. The DEM is then used to derive river geometries. We assume rivers in cells where the upstream area is larger than 1 km^2. Because river bathymetry data are not available, we calculate the river dimensions based on bankfull discharge as described by Sampson et al. (2015), using the 2-year return period value calculated from observed discharge (29.5 m^3/s) with extreme value analysis. We use the Block Maxima method to extract maximum annual discharge and fit a Generalized Extreme Value (GEV) distribution. Using this discharge (Q), we employ power law equations to calculate the width (w) and depth (d), based on Andreadis et al. (2013). Andreadis et al. (2013) also give a 95% confidence interval, which is used to calibrate the river width and depth so that the 2-year return period rainfall event results in no flooding (Equations 1 and 2). We burn in the rivers with their corresponding width and depth in the DEM, resulting in a lower topography in the river channels compared to the unaltered DEM.

$$w = 7.2Q^{0.50} \quad (1)$$

$$d = 0.63Q^{0.31} \quad (2)$$

where w is the river width, d is the river depth, and Q is the bankfull discharge corresponding to a 2-year return period.

3.1.4. Infiltration

An important process to consider in assessing the effectiveness of NBSs, is the infiltration during the event, which is dependent on the soil moisture capacity, the actual soil moisture at the start of the event, and percolation in the soil during the event. We use the infiltration with recovery method within SFINCS, meaning that if no rainfall happens the soil will dry up, creating more storage capacity within the soil. To do so, it requires three input files: the maximum soil moisture storage capacity, the soil moisture storage capacity at the start of the event, and the saturated hydraulic conductivity (Deltares, 2024b). We calculate these inputs using the hydrological module of the GEB model (e.g., De Bruijn et al., 2023) based on the CWatM hydrological model (Burek et al., 2019). In the context of this study, the most notable difference from the original CWatM, is the improved soil water fluxes based on Darcy's law and parameterization of the soil water balance equation derived from soil properties. Soil properties are in turn based on the SoilGrids data set (Poggio et al., 2021a, 2021b), which includes data on soil layer height, organic carbon content, sand content, clay content, and silt content. We determine the saturated water content (which equals the maximum soil moisture storage capacity) using the pedotransfer function developed by Tóth et al. (2015). We calculate the saturated hydraulic conductivity using Brakensiek et al. (1984). The soil moisture storage capacity is calculated for a daily timestep. This is used to indicate the soil moisture storage capacity at the start of the flood event. An example of these input maps is shown in Figure S1 in Supporting Information S1.

3.2. Exposure and Vulnerability

3.2.1. Exposure

Where available, we use object-based data from OpenStreetMap (OSM) to represent buildings, roads, and railways in flood zones (Sieg et al., 2019). OSM data has been reported to be (near) complete for the study area (Barrington-Leigh & Millard-Ball, 2017; Herfort et al., 2023; Oostwegel et al., 2023). The use of OSM data is common in flood risk analysis, demonstrating the suitability of the data for this purpose (e.g., Bubeck et al., 2019; Figueiredo et al., 2020; Koks et al., 2019; Sieg et al., 2019; Sieg & Thieken, 2022). For simulating the exposure of agricultural and natural areas, we use the ESA WorldCover database on a 10 m resolution, as done in similar raster-based flood risk assessment approaches (e.g., De Moel et al., 2011). The data set is resampled to a 5 m resolution for use in SFINCS.

3.2.2. Vulnerability

Figure 3 shows the vulnerability curves used in this study. The vulnerability curve shows the relationship between inundation depth and the damage factor i.e., the fraction of the maximum damage for a certain water depth (e.g., Huizinga et al., 2017). For buildings, we use empirically derived vulnerability curves for the area, based on data collected after the 2021 flood event (Endendijk et al., 2023a). The curves start rising quickly after a 0.1 m water depth (damage ratio 0.5), but then rise more slowly until 5 m (damage ratio 0.8). We chose these curves instead of the commonly used Dutch curves published in Huizinga et al. (2017), because the Huizinga curves were created after the coastal floods in 1953 in the Netherlands, making the data partly outdated and unrepresentative of a riverine flood (De Bruijn et al., 2015; De Moel et al., 2025). The curves by Endendijk et al. (2023a) represent the current vulnerability in the study region for this type of flooding. For roads, we use European vulnerability curves and estimates of maximum damage for different road types (Van Ginkel et al., 2021). For railways, we use Austrian curves and maximum damages from Kellerman et al. (2015), due to the lack of such data for the Netherlands (Nirandjan et al., 2024). For nature and agriculture, we use curves developed by De Moel et al. (2014). For nature, we take into account only clean-up costs as the maximum damage (De Moel et al., 2014).

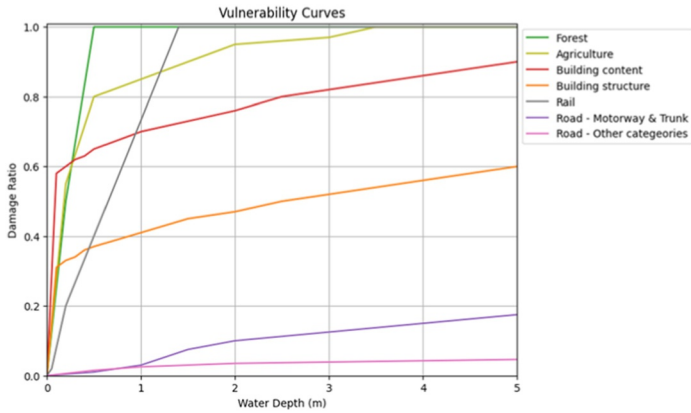

Category	Maximum damage
Forest	0.05 euro / m^2
Agriculture	1.06 euro / m^2
Buildings Structure	1,938.06 euro / m^2
Buildings Content	81,424.50 euro / building
Rail	9,150.39 euro / m
Road - Motorway	5,212.41 euro / m
Road – Trunk	1,303.10 euro / m
Road – Primary	65.16 euro / m
Road – Secondary	32.58 euro / m
Road – Tertiary	13.03 euro / m
Road – Residential & Unclassified	6.52 euro / m

Figure 3. The vulnerability curves (left) used in this study derived from multiple sources. The damage is estimated by multiplying the damage ratio with the maximum damages per category (right).

3.3. Validation

Flood extent: We use maximum flood extents during the July 2021 floods in the Netherlands (Slager et al., 2021), based on remote sensing imagery, and compare this to the simulated flood extent to validate our model. In the simulations, we consider a pixel flooded if water depth exceeds 0.15 m, following Wing et al. (2017). We calculate hits (flooded pixel in both model and observations), misses (flooded pixel in observations, dry pixel in model), and false alarms (flooded pixel in model, dry pixel in observations) (see Table S3 in Supporting Information S1, adapted from Wing et al., 2017).

Hit Rate (HR): The hit rate is the ratio of correctly flooded pixels (higher is better), ranging from 0 (no flooded observation pixels match the flooded model pixels) to 1 (all flooded observations pixels match the flooded model pixels).

$$\mathrm{HR} = \frac{\mathrm{Hits}}{\mathrm{Hits} + \mathrm{Misses}} \tag{3}$$

False Alarm Ratio (FAR): The FAR indicates the ratio of falsely flooded pixels (lower is better), ranging from 0 (no false alarms) to 1 (all false alarms).

$$\mathrm{FAR} = \frac{\mathrm{False\ Alarms}}{\mathrm{Hits} + \mathrm{False\ Alarms}} \tag{4}$$

Critical Success Index (CSI): The CSI balances the hit rate (i.e., underprediction) and the FAR (i.e., overprediction). It can range from 0 (no match between modeled flood and observed flood) to 1 (perfect match between modeled flood and observed flood). A critical success index above 0.7 is considered good model performance (e.g., Bernhofen et al., 2018).

$$\mathrm{CSI} = \frac{\mathrm{Hits}}{\mathrm{Hits} + \mathrm{Misses} + \mathrm{False\ Alarms}} \tag{5}$$

Water depth: Endendijk et al. (2023b) conducted a survey among inhabitants of the flooded area in July 2021 to estimate the water depth on the streets and in houses. Each water depth is reported per 4-digit postal code level (PC4) ($n = 305$). We calculated the average water depth for each postal code. Moreover, we estimated the average simulated water depth of the July 2021 for the same postal codes. For each postal code, we compared the average simulated water depth to the average observed depth. Because not all postal codes have the same number of observations, we calculated a weighted average difference for the entire catchment area, using the number of observations per postal code as weight.

Flood damages: Kok et al. (2023) reported the number of exposed assets and the associated damages after the July 2021 flood based on ENW - Task Force Fact Finding Hoogwater, (2021) for the Netherlands, which we compare to the simulated damages of the same flood event for the Dutch part of the catchment.

3.4. Nature-Based Solutions

We implement three types of NBSs in our model. We focus on these three NBSs because they are currently being considered by the Water Board for implementation:

1. *Retention ponds*: Retention ponds can temporarily store water to reduce the amount of water that flows downstream (Mubeen et al., 2021). There are currently 151 retention ponds in the Dutch part of the catchment (Waterboard Limburg, 2019a). Therefore, we produce a scenario where we create 37 additional retention ponds in Belgium, and increase the storage in the current ponds by making them 1 m deeper. We do not change the spatial extent of the ponds. We choose this configuration so that the current strategy of the water board can be evaluated and better options can be identified. Within the model, we assign a storage volume to each cell. Only once the storage volume is reached, does any extra water contribute to flooding the area.
2. *Reforestation*: Reforestation reduces flood risk through three main mechanisms. First, the porosity underneath a reforested area is greater than underneath a non-forest area, resulting in a larger soil water storage capacity (Moos et al., 2018; Rüegg et al., 2022). Secondly, the saturated conductivity increases, resulting in higher infiltration rates (Moos et al., 2018; Rüegg et al., 2022). Lastly, the water flow velocity is reduced by increased hydraulic overland flow resistance (Moos et al., 2018; Rüegg et al., 2022). The first two mechanisms (porosity and saturated conductivity) are implemented by developing new soil property maps, that change the bulk density and soil organic carbon content in the topsoil layers for the reforested areas (see Figures S2 and S3 in Supporting Information S1). Increased evapotranspiration is modeled in the hydrological model by changing the land use from the original land use to forest. The increased flow resistance is implemented in the model by changing the Manning's roughness coefficient to 0.12 following Dixon et al. (2016) and Table S2 in Supporting Information S1. Our scenario consists of expanding the current forested area by 10%, in line with Dutch policy plans for the region (Provincie Limburg, 2022). This corresponds to 10 km^2 of reforested areas. We convert cropland and grassland to forest on hills steeper than 10% because these hills tend to be less suitable for agriculture (e.g., Bandyopadhyay et al., 2009, see also Table S5 in Supporting Information S1). We assume our forest is 100 years old, similar to the oldest forests found in the catchment (Besnard et al., 2021).
3. *Conversion of cropland into natural grassland*: Conversion of cropland into grassland changes flood risk through mechanisms similar to those of reforestation. Firstly, grasslands have 25%–32% higher infiltration rates than cropland (Strock et al., 2022). Secondly, the soil water storage capacity increases, because of higher porosity (Wu et al., 2016). We implement these mechanisms by decreasing bulk density and increasing soil organic carbon content in the topsoil layers (Figures S4 and S5 in Supporting Information S1). These changes have also been found by Strock et al. (2022) and Wu et al. (2016) using field experiments. It is important to note that these changes are smaller than for the reforestation scenario. There are currently no plans by local governments to implement this NBS. Therefore, we convert 10 km^2 of cropland on slopes steeper than 2% into grassland (see also Table S6 in Supporting Information S1). Using the same total surface area allows for comparison with the reforestation scenario.

3.5. Building-Level Adaptation Measures

We develop two building-level adaptation scenarios: wet- and dry-proofing. We implement these measures in the model using the information from Endendijk et al. (2023a). Recall that vulnerability curves [0–1] express the relative damage as a fraction of the maximum possible damage for a given flood depth. For wet-proofing, we shift the curve down with 0.203 for building structure and 0.382 for building content (Endendijk et al., 2023a), each with a minimum of 0. Buildings cannot be safely dry-proofed above 1 m, because the water pressure resulting from higher water levels would reduce the structural integrity of buildings (Mortensen et al., 2024). Therefore, we assume that no damage occurs for the first meter of flooding in our dry-proofing scenario (as done in de Moel et al., 2014; Mortensen et al., 2024). The adapted curves can be seen in Figure S6 in Supporting Information S1. We assume that all households in the floodplain implement these measures. However, from survey data we know that the current implementation rate is around 6%–18% (Endendijk et al., 2023b).

3.6. Evaluation of Measures by Comparing Adaptation Scenarios

We compare five adaptation scenarios (three NBSs and two building-level; Section 3.4 & 3.5) with a baseline scenario where no additional measures are implemented. To compare the effectiveness of each adaptation scenario for flood risk reduction, we use seven different evaluation criteria: expected annual damage (EAD), effect on damages, effect on flood extent, effect on average water depth, implementation costs, net present value (NPV), and the benefit-cost ratio (BCR). For estimating the EAD and damages we consider the full range of return periods (25, 50, 100, 200, 250, 500, and 1,000 years). For the effect on flood extent and average water depth, we consider the effects for three return periods—25, 100, and 1,000 years—to cover the range from smaller, more frequent floods to larger, less frequent floods.

Expected Annual Damage (EAD): We calculate the EAD for all scenarios using Equation 6 following Ruangpan et al. (2024). We use the trapezoidal rule to provide a numerical approximation of the continuous integral.

$$\mathrm{EAD} = \int_{f=0}^{\infty} \mathrm{Damage}(z_f)\, df \tag{6}$$

where f is the exceedance probability and Damage is the flood damage caused by water level z_f during an event with an exceedance probability f.

Damage: We calculate the damage for all scenarios. We use Equation 7, modified from Zeleňáková et al. (2020), to calculate the damage to a specific object, and calculate the sum to obtain total damage.

$$\mathrm{Damage} = \sum_{i,k} E_{i,k} * \mathrm{MaxDam}_{i,k} * \mathrm{DR}_{d,k} \tag{7}$$

Where i is an object in land use category k. $E_{i,k}$ is the exposed area for object i in category k, $\mathrm{MaxDam}_{i,k}$ is the maximum damage for object i in category k, and $\mathrm{DR}_{d,k}$ is the damage ratio corresponding to a certain water depth d for category k.

Flood extent: We calculate flood extent as the total number of flooded cells multiplied by the model resolution for all scenarios for three return periods (e.g., Lallemant et al., 2021).

Average water depth: We calculate the average water depth as the mean depth across all flooded cells for all scenarios for three return periods (e.g., Ferreira et al., 2020).

Costs: We compare the investment costs of all adaptation scenarios. An overview of the implementation costs used in the study can be found in Table S5 in Supporting Information S1. We collected this information from local governments, as well as the literature. All monetary values were converted to 2024 euros to account for inflation. Land acquisition costs are estimated to be around € 91,300/ha (Kadaster, 2025).

Net Present Value (NPV): We calculate the net present value (NPV) for all five adaptation scenarios using Equation 8 following Ruangpan et al. (2024). The NPV gives an indication of the total net benefits an investment generates. If the NPV is positive, the investment is expected to generate more benefits than costs. Conversely, a negative NPV reflects that the investment will generate more costs than benefits.

$$\mathrm{NPV} = \sum_{t=0}^{T} \frac{\mathrm{EAD}_{t,\mathrm{baseline}} - \mathrm{EAD}_{t,\mathrm{measure}}}{(1+r)^t} - \left(\mathrm{CC} + \sum_{t=0}^{T} \frac{\mathrm{MC}_t}{(1+r)^t}\right) \tag{8}$$

where the benefits and costs are summed over the time horizon (T) of the project, $\mathrm{EAD}_{t,\ \mathrm{baseline}}$ is the EAD of the baseline scenario in year t, $\mathrm{EAD}_{t,\ \mathrm{measure}}$ is the EAD of the adaptation scenario in year t, r is the discount rate, CC are the construction costs and MC are the maintenance costs. We use a time horizon of 30 years and a discount rate of 3% following the guidelines of the European Union for infrastructure projects (European Commission, 2021).

Benefit-Cost Ratio (BCR): We calculate the BCR for all five adaptation scenarios using Equation 9 following Ruangpan et al. (2024). The BCR gives an indication of the benefits generated per specific unit of investment. A BCR above 1 indicates that the benefits are expected to outweigh the costs.

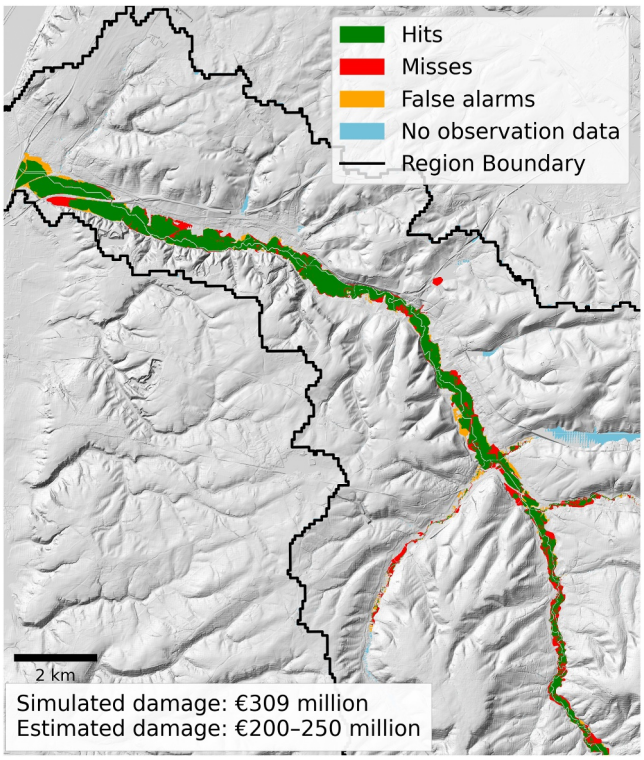

Figure 4. Flood map of a part of the Geul catchment comparing the simulation of the 2021 floods with the observation data. We show hits in green, misses in red and false alarms in orange. For some side streams, no observations were available; these are marked in blue.

$$\mathrm{BCR} = \frac{\sum_{t=0}^{T} \frac{\mathrm{EAD}_{t,\mathrm{baseline}} - \mathrm{EAD}_{t,\mathrm{measure}}}{(1+r)^t}}{\mathrm{CC} + \sum_{t=0}^{T} \frac{\mathrm{MC}_t}{(1+r)^t}} \quad (9)$$

where the notation is the same as in Equation 8.

4. Results

4.1. Model Validation for 2021 Event

We validated the modeled flood extent on the flood extent observed during the July 2021 flood event. We find an average CSI of 0.74 over the catchment area, indicating good model performance (e.g., Mester et al., 2021). The model performs best downstream, capturing almost all observed flooded pixels (Figure 4). In the upstream tributaries, the model performs less well (CSI ranging from 0.15 to 0.47, an extensive analysis can be found in S1.9), producing more false alarms and misses. However, this could also partly be explained by uncertainty in the flood observation data, which were manually delineated using flood marks from aerial pictures taken after the water had subsided (ENW - Task Force Fact Finding Hoogwater, 2021). Note that for some of the upstream rivers no observation data were available.

We also compared our simulated flood depth (see Figure S8 in Supporting Information S1 for a histogram of simulated water depth) to survey observations (Endendijk et al., 2023b) to determine whether the observed and simulated values fall in the same range. The survey respondents estimated water depth in 5 classes: <0.2, 0.2–0.5, 0.5–1, and >2 m (Endendijk et al., 2023b). This estimation was then translated into a water depth by Endendijk et al. (2023b). Respondents reported an average water depth of 0.53 m outside on the street. When we compare the weighted difference between observations and simulations, the differences range from an underestimation of 0.19 m up to an overestimation of 0.55 m. When we calculate an average weighted difference, we arrive at a difference of 0.24 m. This relatively small difference provides confidence that our model simulates realistic water depths, especially considering that both data sets are associated with uncertainty. One of these uncertainties is the estimation of observed water depth. Since the water depth class intervals are broader than our difference of 0.24 m, we conclude that the model simulates realistic water depths.

Lastly, we compared our simulated damages to estimated damage and insurance claims. From our model we find damages of approximately €309 million for the Dutch part of the Geul catchment. This is in the same order of magnitude as the estimated €200–250 million by Kok et al. (2023) and ENW - Task Force Fact Finding Hoogwater (2021). The €200–250 million was estimated using the SSM-2017 model (Slager & Wagenaar, 2017). This model uses vulnerability curves for building content and structure, which were been developed using data primarily from the 1953 coastal flood in the Netherlands (De Bruijn et al., 2015). Since the flood in the Geul was a riverine flood, these curves are less suitable to our case study compared to the curves developed by Endendijk et al. (2023a). Considering these uncertainties in the SSM-2017 model, this difference in damage is acceptable and a strong indication of the high quality of our model. A comparison of our total losses with insurance claims shows that the insurance claims are much lower (€43 million). This difference can be explained because: (a) a significant amount of damage (around 40%) was not compensated by insurance companies (Endendijk et al., 2023b; Kok et al., 2023); (b) insurance companies use depreciated values for building structure and content damages, while we use replacement cost values in this study (Endendijk et al., 2023a); and (c) the insurance claims were only for homeowners with insurance, while we also include simulated damage for infrastructure, the entire building stock, agriculture and nature.

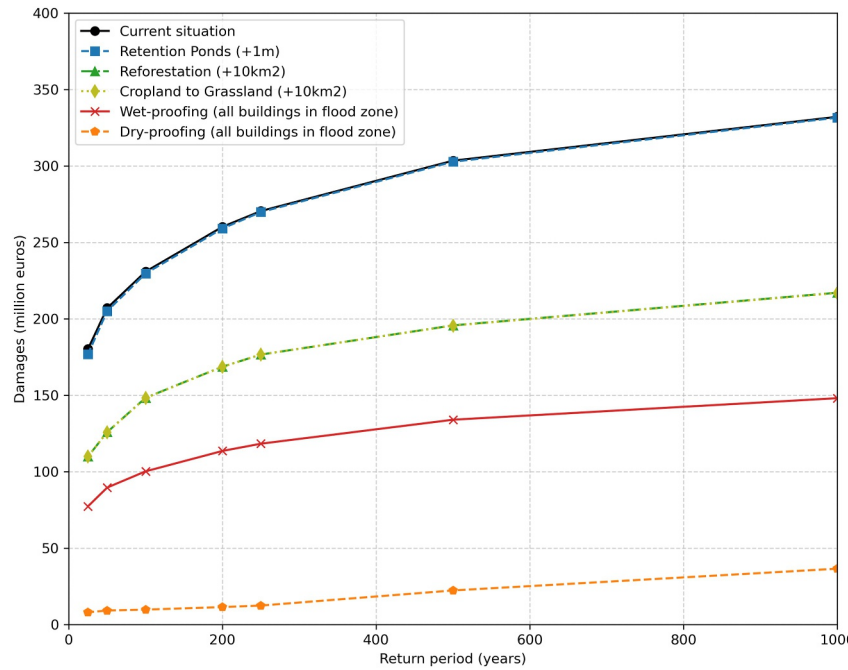

Figure 5. Damages per return period for each of the adaptation scenarios.

4.2. Evaluation of Adaptation Measures

We evaluated our adaptation measures using estimates of the damage for seven different return period events. Figure 5 shows the damage per return period. The current situation is shown in black. For the current situation, damages are approximately €180 million for a return period of 1 in 25 years (see also Table 1). For the largest

Table 1
An Overview of the Effectiveness of the Selected Adaptation Measures

	Return period	Current situation	Retention ponds (+1 m)	Reforestation (+10 km^2)	Cropland to grassland conversion (+10 km^2)	Wet-proofing (all buildings in flood zone)	Dry-proofing (all buildings in flood zone)
EAD [Meuro/yr]	–	8.45	8.37	5.27	5.27	3.66	0.40
Damage [Meuro]	25	180	177	110	110	77	8
	100	231	230	148	148	100	10
	1,000	332	332	217	217	148	37
Flood extent [km^2]	25	6.06	5.88	5.34	5.34	6.06	6.06
	100	6.92	6.78	6.20	6.20	6.92	6.92
	1,000	8.51	8.38	7.46	7.46	8.51	8.51
Average water depth [m]	25	0.48	0.47	0.43	0.43	0.48	0.48
	100	0.53	0.53	0.47	0.47	0.53	0.53
	1,000	0.63	0.62	0.54	0.54	0.63	0.63
Benefits [Meuro/yr]	–	–	0.78	3.17	3.18	4.78	8.05
Costs [Meuro]	–	–	9.9	16.8–108.1	11.2–102.5	86.6	135.4
NPV [Meuro]	–	–	−8.3	−45.8–45.5	−43.6–47.9	12.0	30.5
BCR	–	–	0.16	0.59–3.28	0.60–3.72	1.14	1.23

Note. For every measure the EAD, damage, flood extent, average water depth, benefits, costs, NPV and the BCR are reported. For reforestation and cropland to grassland conversion, we provide a cost range for only the implementation costs (lower bound) and including land acquisition costs (upper bound), translating into a range for NPV and BCR.

return period (1 in 1,000 years) damages are estimated to reach approximately €330 million. By implementing an adaptation measure, the damage can be reduced substantially. For the 1/25 and 1/100 events, only a small reduction in losses is observed when implementing retention ponds with damage reduction of €3 million and €1 million compared to the current situation, respectively. For more extreme floods (<1/100 years), retention ponds do not lower losses compared to the current situation. The NBS scenarios of reforestation and cropland to grassland conversion perform similarly, reducing damage by 35%–39% depending on the return period. The damage reduction is largest for the 1/25 event with 39% damage reduction, and smallest for the 1/1,000 years event with 35% damage reduction. NBSs are therefore most effective for the more frequent, smaller-scale floods. The building-level adaptation scenarios outperform all NBSs, with dry-proofing reducing more damage than wet-proofing: dry-proofing can reduce damage up to 95%, while wet-proofing reduces around 55% of the damage.

Table 1 presents a broader evaluation of the adaptation scenarios using different metrics: damage estimations (a breakdown of damage per sector can be found in S7), EAD, flood extent, average water depth, benefits, costs, NPV, and the BCR. Reforestation and cropland to grassland conversion have the largest effect on the physical properties of the flood, reducing flood extent by 12% and average water depth by 10% for the 1-in-25-year flood. Retention ponds, in comparison, have a much smaller reduction in flood extent (3%) and flood depth (0.5%) for the same flood; not all flood water encounters a retention pond and storage is limited. The dry-proofing and wet-proofing scenarios do not change the physical properties of the floods. It is important to note that not all measures have the same size. The reforestation and cropland to grassland conversion both require large areas of land to be converted (10 km^2), while the retention ponds scenario is implemented on a much smaller scale by deepening existing ponds by 1 m and only installing 37 new ponds. From Table 1, we can conclude that large-scale measures have more benefits than small-scale measures.

We observe a major difference in the implementation costs of the adaptation measures. Expanding the retention ponds is the cheapest option requiring €9.9 million. When land acquisition costs are not included, the other NBSs cost only slightly more: €16.8 million for reforestation and €11.2 million for cropland to grassland conversion, respectively. However, if we include land acquisition costs, the total costs rise to €108 million for reforestation and €103 million for cropland to grassland conversion. Building-level adaptation measures, however, are much more expensive. For these scenarios, around 3,000 houses in the flood zone need to be adapted, resulting in costs of €86.6 million for wet-proofing and €135.4 million for dry-proofing.

However, the resulting benefits are also important. Therefore, we weigh costs against benefits. For this analysis, we use the NPV and BCR, which are widely used metrics in flood adaptation decision-making (e.g., Aerts et al., 2014; De Ruig et al., 2019). The NPV is highest for reforestation and cropland to grassland conversion (excluding land acquisition costs). The NPV becomes negative when including land acquisition costs, reflecting uncertainty regarding the economic attractiveness of these measures. Wet-proofing results in a much smaller NPV (€12.0 million) than dry-proofing (€30.5 million). The expansion of the retention ponds has an NPV of -€8.3 million, which is negative but still higher than the NPV for the other NBSs when including land acquisition costs. The BCR is highest for reforestation (3.28) and cropland to grassland conversion (3.72), but if we include land acquisition costs, the BCR drops below one to 0.59 and 0.60, making these adaptation scenarios not economically attractive. The retention ponds are economically unattractive with a BCR of 0.16. The two building-level adaptation measures are both economically attractive options with a BCR just above one: 1.14 for wet-proofing and 1.23 for dry-proofing.

4.3. Upstream-Downstream Dynamics

Figure 6 shows the spatial differences in the EAD, total economic value, and spatial effects of two adaptation scenarios. We chose to focus on only reforestation and dry-proofing because the other three adaptation measures show similar spatial patterns (see Figure S9 in Supporting Information S1). The EAD in the current situation is the highest in the downstream municipalities such as Meerssen, Valkenburg aan de Geul and Gulpen-Wittem. When comparing this map with the total asset value in those areas, we see that these municipalities have high asset values, but there are other upstream municipalities with high asset values as well (e.g., Plombières, Vaals and Kelmis). However, these upstream municipalities have less risk of flooding because of their upstream location with lower flood depths in the simulations.

An examination of the benefits of the different adaptation scenarios, reveals several patterns. For the reforestation scenario, the municipality that benefits most is Gulpen-Wittem, which is the municipality in which several

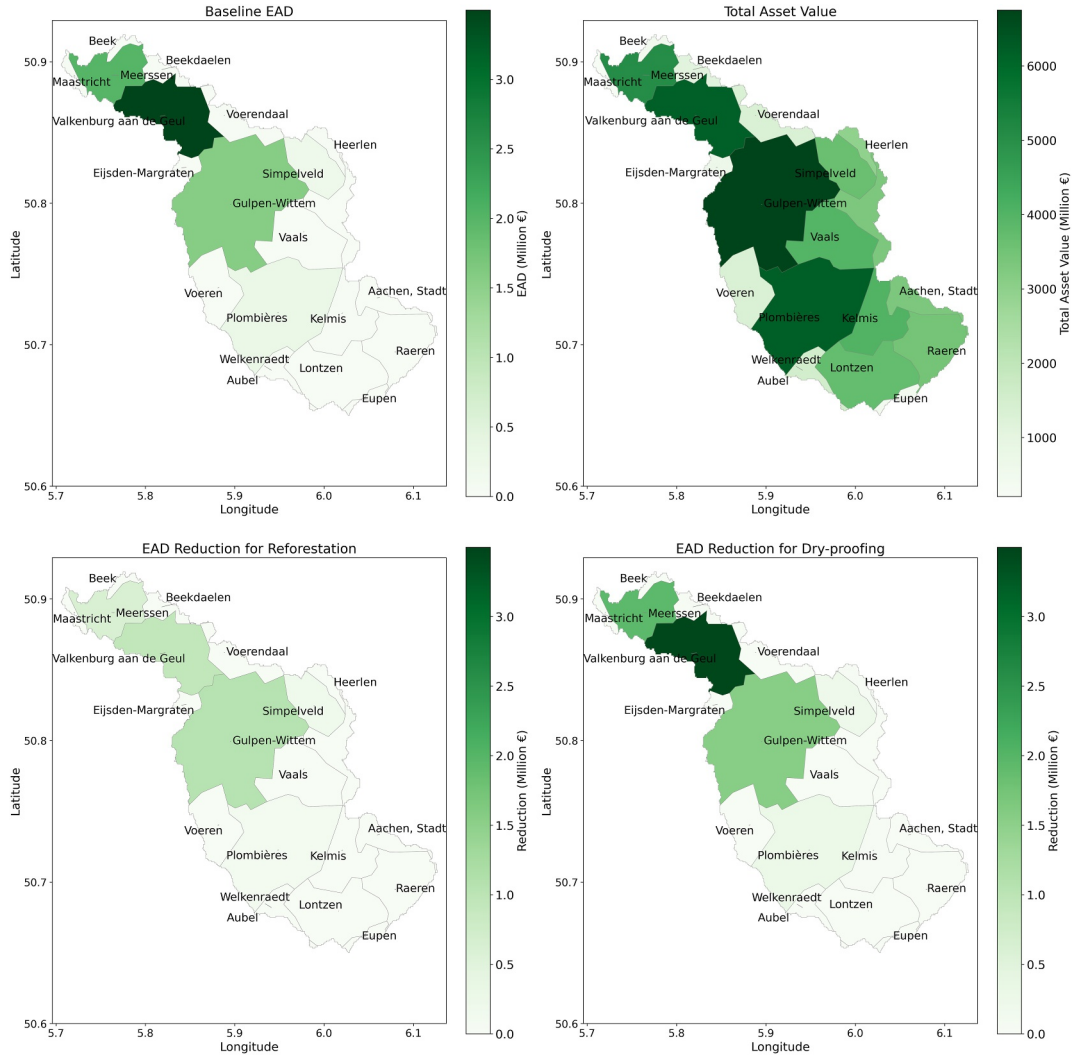

Figure 6. Spatial analysis of expected annual damage (EAD) for all the municipalities located in the Geul catchment, with the current EAD (top left panel), total economic value (top right panel), the EAD after reforestation (bottom left panel), and the effect of dryproofing (bottom right panel).

tributaries confluence into the main branch of the Geul. This region lies at the border between the upstream and downstream municipalities. Nevertheless, the downstream municipalities, such as Valkenburg aan de Geul and Meerssen, also benefit from the reforestation scenario. The municipality of Simpelveld also has a higher damage reduction, being one of the municipalities where some of the forest is created. In the dry-proofing scenario, the municipalities with the largest share of buildings also have the largest share of EAD. Therefore, when reducing the damage to buildings, we observe the same pattern with the most risk reduction occurring in urbanized areas. In conclusion, implementing building-level adaptation measures has the largest benefits in municipalities with many buildings: in this case, the downstream communities. NBSs are most effective where they are implemented, in our case upstream, but also reduce some of the EAD in downstream communities.

4.4. Effectiveness for the 2021 Flood

When focusing only on the 2021 event (thus not on other floods with other return periods as in the previous sections), our results are mostly in line with the findings presented in Sections 4.1–4.3 (Figure 7). However, the retention pond scenario seems even less effective. Only around €1 million of damage could have been prevented. This can be explained by the mismatch between the location of the heaviest rainfall (upstream, in the Belgian part of the catchment) and the location of the majority (80%) of the retention ponds (downstream, in the Netherlands).

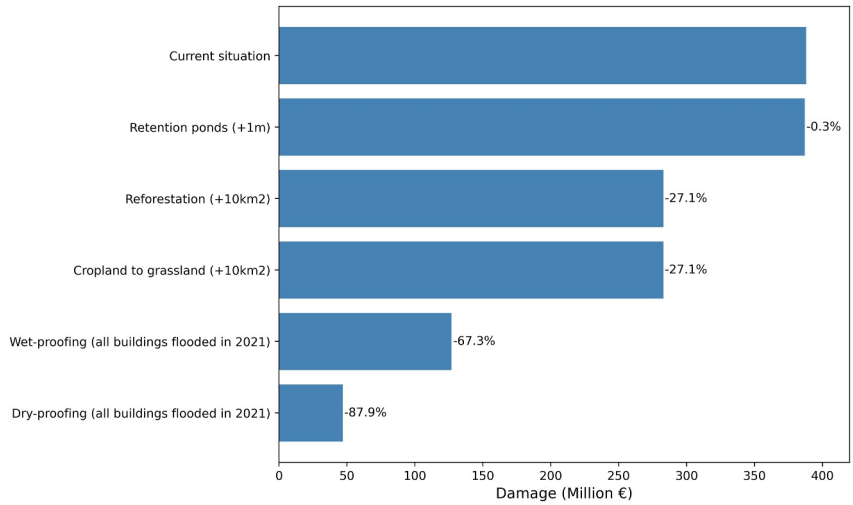

Figure 7. The damage reduction of each adaptation scenario for the July 2021 flood.

Therefore, most rainwater never passed the retention ponds on the way to the river, resulting in high discharge. Reforestation and cropland to grassland conversion yield similar outcomes. For both NBS scenarios, the locations of the land use changes are upstream in the catchment, where most rainfall fell during the 2021 event. Therefore, reforestation would have been an effective strategy for this specific event by slowing down discharge and enhancing soil infiltration. By far the most effective are the building-level adaptation measures, with dry-proofing having the best results. In our modeled results, around 3,800 buildings were flooded for this specific flood, but only 210 of them had water depths greater than 1 m. By implementing dry-proofing until 1 m, most buildings are protected. Therefore, dry-proofing is the most efficient way to reduce damage for this particular event.

5. Discussion

5.1. Nature-Based Solutions

This study shows that several adaptation measures can effectively reduce flood risk. Our results indicate that expanding the current retention ponds is economically inefficient with low BCRs. Currently, there is a storage capacity of around 0.7 million m^3, which is expanded to around 1.7 million m^3 in the retention ponds scenario. In comparison, the rainfall events we use result in 30 million (1-in-25-year event) to 54 million (1-in-1,000-year event) m^3 of water flowing downstream. Therefore, it is intuitive that this scenario reduces flood risk only marginally. In order for the retention ponds to be effective, much more storage capacity has to be implemented in the catchment. Ruangpan et al. (2024) find a much larger flood risk reduction (−32%) for retention ponds in the Tamnava basin in Serbia, which results in a BCR of 0.5. The retention ponds used in their study have a capacity of 14.2 million m^3, while the catchment is around 726 km^2. In our case, this is 1.7 million m^3 relative to a surface area of 340 km^2, which is roughly four times lower retention capacity relative to the size of the catchment. Retention ponds can have more efficient results if their storage capacity is increased. For example, if we make all retention ponds the size of the current largest pond in the catchment, the total storage capacity will be 11.75 million m^3. This can reduce flood damages by up to €20 million (−11%) for a 1-in-25-year event. Therefore, we can conclude that the size and location of the retention ponds is essential to consider when designing flood adaptation scenarios.

The results for reforestation show a large decrease in EAD (−38%). Ruangpan et al. (2024) also model a reforestation scenario of +1,409 ha in a catchment of 726 km^2 and find a risk reduction of −11%. This can be explained by the difference in reforestation: in our scenario, we convert 1,000 ha into forest, which is around 3% of the total catchment, while in Ruangpan et al. (2024) around 2% of the catchment is reforested. The BCR in Ruangpan et al. (2024) is approximately 0.6, which is very similar to our results when we include land acquisition costs (0.59). Ruangpan et al. (2024) highlighted that it is important to include co-benefits of NBSs, such as recreation and biodiversity values, and demonstrated that by including co-benefits BCRs often rise. We estimate the co-benefits for reforestation to be valued around 13.3 million euro per year using the value transfer function

developed by Garcia Alvarez et al. (2025). If we include these co-benefits in our CBA, the BCR increases from 0.59 to 3.06 (including land acquisition costs), clearly illustrating the sensitivity of economic evaluations to the inclusion of non-market benefits. This finding underscores that evaluations based solely on avoided flood damages may underestimate the broader societal value of NBSs, particularly in terms of ecosystem services, biodiversity conservation, and long-term climate adaptation. Future research could further refine these estimates by applying site-specific economic valuation methods for NBS co-benefits in the Geul catchment. Incorporating such benefits would allow for a more comprehensive assessment of adaptation strategies and may alter the relative ranking of measures.

There are some uncertainties in the modeling of NBSs. In this study we assumed that the NBSs would be immediately effective when implemented at $t = 1$. However, the effectiveness of reforestation against flooding increases with forest age (Archer et al., 2016). Older forests have higher infiltration rates and larger porosity (Archer et al., 2016; Zema et al., 2021). Zema et al. (2021) show that forests older than 80 years have the highest hydraulic conductivity. Therefore, the CBA we performed is a simplification of reality: in real life the benefits of reduced flooding gradually increase, instead of being fully effective at timestep 1. Nevertheless, Keesstra et al. (2018) show that most soil improvement already occurs in the first 5–10 years after land abandonment. Therefore, we can conclude that at least part of the flood risk reduction benefits are already in place after 5–10 years for both reforestation and cropland to grassland conversion. It should be noted that for gray measures as well, the implementation time can be several years (Vikolainen et al., 2013), for example, due to the time spent on planning, obtaining permits, and construction. Moreover, while interception and evaporation are included in the hydrological model to obtain the conditions at the start of the event, these processes are not included in our hydrodynamic model. In the UK, an average of 10%–25% of annual rainfall is intercepted by broadleaf forests (Nisbet, 2005). However, there is still ongoing debate about the amount of rainfall that can be intercepted during a high-intensity rainfall event (i.e., the total canopy storage, Cooper et al., 2021). There is general consensus that once the total canopy storage volume is reached, the rest of the rain will become throughfall (Cooper et al., 2021; Link et al., 2004). Moreover, evaporation rates become very low during rain because of a low humidity deficit and low radiation due to clouds (Klaassen et al., 1998). Therefore, we assume that during our high-intensity rainfall events interception and evaporation play a limited role. Future research could further assess possible effects.

Moreover, there is uncertainty in the soil parameters used in our analysis (see Section 3.1.4), particularly in the saturated hydraulic conductivity and the antecedent soil moisture conditions prior to heavy rainfall events. We performed a sensitivity analysis to assess how these parameters influence our results (see S.1.14). These results show that the outcomes are not very sensitive to changing saturated hydraulic conductivity, with a damage range between −0.25% less damage and +0.07% more damage. Antecedent soil moisture conditions play a larger role in sensitivity. If the soil is completely dry, damages can be up to 10% lower because the flood is less severe due to increased water storage in the soil. Conversely, if the soil is completely saturated, damages can be up to 10% higher due to a more severe flood. However, this effect is strongest for the 1-in-25-year event and has almost no influence for the 1-in-1,000-year flood event. This is most likely due to the extreme precipitation associated with such events, for which infiltration plays a much smaller role. Moreover, even when accounting for uncertainty, damage reduction remains substantial (56–80 million euros for the 1-in-25-year event), clearly exceeding uncertainty linked to soil parameters. We also incorporated our newly derived sensitivity bounds of the EAD into the CBA (see Table S14 in Supporting Information S1). The results indicate that BCR outcomes remain relatively stable, ranging from 0.55 to 3.40 for reforestation and from 0.56 to 3.85 for cropland to grassland conversion. Therefore, we conclude that uncertainty in the soil parameters does not affect the main findings of this study.

5.2. Building-Level Adaptation Measures

Our results show that dry-proofing is more effective than wet-proofing, with a flood risk reduction of 95% versus 55%. This is in line with the findings of De Moel et al. (2014), who showed a risk reduction of 61% for dry-proofing and 29% for wet-proofing. Both our case study and De Moel et al.'s (2014) show average inundation depths up to 1 m. Yet, the flood risk reduction effect is larger in the Geul case study compared to De Moel et al. (2014) because the share of EAD explained by building losses is around 95%, which is larger than in De Moel et al. (2014)'s case (around 85%).

Based on survey results from the Geul region, Endendijk et al. (2023a) find flood damage reduction of 30%–40% for dry- and wetproofing measures combined, while we find a reduction of 67%–88%. However, in our modeling

study, we assume perfectly working measures, while two thirds of the survey respondents reported that placed sandbags or flood shields were either not high enough or strong enough to prevent water from entering the building (Endendijk et al., 2023b). Nevertheless, Endendijk et al. (2023a) also conclude that dry-proofing is more effective than wet-proofing in this area because of predominant inundation depths below 1 m in urban areas. Moreover, we assume in our study that all inhabitants in the 1-in-1,000-year flood zone implement floodproofing measures. However, in reality, we see that only 6%–18% of people living in the area (Endendijk et al., 2023b) have taken structural floodproofing measures. In order to improve the uptake, it is important to understand the constraints to flood adaptation to obtain a realistic estimation of how much flood risk reduction can be realistically be expected through these measures: that is, it is necessary to understand the limits of flood adaptation through household behavior (Aerts et al., 2024).

5.3. Model Innovations and Limitations

In our study, we extended the open-source socio-hydrological model GEB (de Bruijn et al., 2023) with a hydrodynamic, and flood risk model. Such a model did not previously exist. For example, Ferreira et al. (2020) manually couple the hydrologic HEC-HMS and the hydraulic HEC-RAS model but do not couple this to a flood risk model. Similarly, Vojinovic et al. (2021) use the hydraulic model MIKE URBAN and hydrodynamic model MIKE FLOOD but also do not couple this to a flood risk model. In contrast, Lallemant et al. (2021) use a similar setup to ours, with their own hydrologic model, the hydraulic model LISFLOOD-FP, and damage model OpenProFIA. However, their setup is not integrated within a single modeling framework. Ruangpan et al. (2024) develop a similar approach with the hydrological HEC-HMS and hydrodynamic model HEC-RAS and couple this to their own flood risk model. However, this setup is not available open source. Our model makes it possible to model the effectiveness of several flood risk adaptation measures within one modeling framework, making it quick and easy to compare several measures with each other. In addition, the fully open-source nature of the modeling framework is particularly advantageous for transboundary catchments such as the Geul, where flood risk management involves multiple jurisdictions. The open-source implementation ensures full transparency regarding the data used and the representation of processes, thereby facilitating collaboration between countries. Furthermore, the model is developed to use global data sets, which reduces inconsistencies arising from differences in national data standards, data availability and spatial resolution. This also accelerates model setup for new regions, which is especially beneficial in transboundary settings. Moreover, there is also support for manually adding local data sets, such as DEM data.

Nevertheless, although our model presents several innovations, there are also several sources of uncertainty, since our model is based on a combination of several models that are associated with uncertainties. For example, creating return period maps based on rainfall data may introduce uncertainty. Vangelis et al. (2022) show that a 50-year return period flood corresponds to a rainfall return period of 110 years. However, this mismatch decreases for smaller catchments and catchments with rapid hydrological responses, which is also the case for the Geul (Viglione & Blöschl, 2009). Another source of uncertainty is hydrodynamic modeling stemming from the input data such as river bathymetry, the DEM, and surface roughness estimates (Teng et al., 2017). Moreover, the SFINCS model has so far mainly been used to simulate coastal floods (Leijnse et al., 2021; Parodi et al., 2020; Röbke et al., 2021; Sebastian et al., 2021), while we use the model for riverine flooding. To ensure that our SFINCS model provides valid results, we validated our model against the 2021 observations. We calculate a CSI of 0.74, showing that our model performs well. There are also uncertainties associated with damage calculations, such as the data on exposed assets as well as the corresponding vulnerability curves, which also affect flood risk estimations (De Moel & Aerts, 2011; Merz & Thieken, 2009). However, relative differences in flood risk have been found to be robust, that is, the relative flood risk reduction remains similar across different combinations of input data (Bubeck et al., 2011; De Moel & Aerts, 2011). Moreover, during our validation process, we showed that our model produces damage estimations similar to those observed during the 2021 flood. Therefore, we are confident that our results provide a reasonable estimate of the possible flood risk reduction achieved through these adaptation measures.

Lastly, we performed an uncertainty analysis with the two most uncertain parameters from our analysis: river depth and the vulnerability curves for buildings (for more see S.1.13). Our results show that changing river depth by 10% can change EAD estimates by 4%–6% (Table S8 in Supporting Information S1). We used these new estimates in our CBA and show that BCRs are robust to these uncertainties in EAD (Table S9 in Supporting Information S1): ratios change slightly but if they were above 1 in the original analysis they remain above 1 in the

uncertainty analysis. Therefore, we can conclude that uncertainties coming from the hydrodynamic model do not largely affect the conclusions from this paper. Changing vulnerability curves, however, has a larger effect on our estimates: EAD decreases by 27%–89% because damages decreased for every return period (Table S8 in Supporting Information S1). Using the new EAD estimates, BCRs dropped below 1 for all tested scenarios. Consequently, it raises the question whether any of the measures are economically attractive to be implemented in the region. However, the relative ranking between the measures persists: thus, building-level measures remain more economically efficient than NBSs. This finding gives confidence in the overall conclusions of the paper that building-level measures are more effective for this catchment than NBSs.

6. Conclusions

In this paper, we evaluated the effectiveness of building-level adaptation measures with nature-based solutions (NBSs) in reducing flood risk. We extended the coupled socio-hydrological model GEB (de Bruijn et al., 2023) with a hydrodynamic and flood risk model, which we published open source. Our coupled model allows for a detailed object-based assessment of flood risk impacts, which we use to evaluate the effect of building-level adaptations and the effect of NBSs. We combined the risk reduction estimates with cost estimates to perform a CBA. We applied our method to the Geul catchment in the south of the Netherlands, bordering Belgium and Germany. The building-level measures are dry- and wet-proofing, and we also tested three NBSs: retention ponds (1 m deeper + 37 new ponds), reforestation (10 km^2), and the conversion of cropland to natural grassland (10 km^2).

The results show that reforestation and conversion of cropland to grassland have the largest effect on the physical properties of the flood, reducing flood extent by 12% and average water depth by 10%. Retention ponds, in comparison, result in a much smaller reduction in flood extent (3%) and flood depth (0.5%), as, given the modeled number and distribution of ponds, they are limited in the amount of water they can store during heavy rainfall events. The building-level adaptation scenarios outperform all NBSs, with dry-proofing reducing more damage than wet-proofing: dry-proofing can reduce damage up to 95%, while wet-proofing reduces around 55% of the damage. The outcomes of the cost-benefit analysis show that dry-proofing (BCR = 1.23) and wet-proofing (BCR = 1.14) are the most economically attractive options, while NBSs remain difficult to monetize due to uncertainties in land acquisition costs and a wide-range of co-benefits.

Our model is a new addition to the well-known published such as HEC-HMS, HEC-RAS, and MIKE FLOOD. It has several innovations: (a) it is published open source, (b) it has an integrated setup consisting of a hydrological, hydrodynamic, and flood risk model, (c) it is a high-resolution (5 m) and high-quality (CSI = 0.74) flood model and, (d) it makes it possible to model both the impacts of building-level adaptation measures and NBSs within one model setup. Future research may further improve our approach. While our model is validated with a CSI of 0.74 (for flood extent), our setup has some sources of uncertainty. For example, we assume that the rainfall return period equals the discharge return period. Further research can test whether this relationship holds true for the Geul River. Furthermore, new research on the co-benefits of NBSs will allow for including those benefits in a more holistic CBA analysis. Moreover, although our estimates show that building-level measures are more effective than NBSs, it remains to be seen whether households will implement such measures at large scales. Future research can develop our model further by combining it with a dynamic agent-based model that simulates heterogeneous adaptation decisions of households. In this way, we can include human behavior in the modeling approach to provide a more realistic estimation of how much flood risk reduction can be achieved through these measures and how this behavior may be affected by various policies. Moreover, we invested in the creation of an integrated open-source modeling chain so that future research can apply our approach to other catchments in the world. These applications will reveal whether our results hold in other contexts, such as in catchments with other sizes, topographies, land uses, or climatic conditions.

Conflict of Interest

The authors declare no conflicts of interest relevant to this study.

Data Availability Statement

All model inputs, code, and results of the GEB model used for this paper are preserved at https://doi.org/10.5281/zenodo.15488420 (Bril et al., 2025) available via GNU General Public License v3.0 and developed openly at https://github.com/GEB-model. The ESA Worldcover data set can be accessed at Zanaga et al. (2022). The SoilGrids data set developed by Poggio et al. (2021a, 2021b) is available at https://files.isric.org/soilgrids/latest/. OpenStreetMap data is available at https://www.openstreetmap.org/. The flood extents used for validation can be found at Slager et al. (2021). Aside from the GEB model, we use the other software programs: Hydro-MT (Eilander, Boisgontier, et al., 2025), HydroMT-SFINCS (Eilander, de Goede, et al., 2025) and SFINCS (van Ormondt et al., 2025).

Acknowledgments
This work is part of the Perspectief research programme Future flood risk management technologies for rivers and coasts with project number P21-23. This programme is financed by Domain Applied and Engineering Sciences of the Dutch Research Council (NWO). This project also received funding from the ERC-COASTMOVE project nr. 8888442. W.J.W. Botzen received funding from the EU ERC INSUREADAPT (Grant Nr. 101086783) and the project NATURANCE (Grant Nr. 101060464) of the Horizon 2020 Framework Programme of the European Union. We kindly acknowledge sponsoring by the VU HPC Council and the IT for Research (ITvO) ADA Linux computational cluster at the VU Amsterdam.

References

Aerts, J. C., Botzen, W. W., Emanuel, K., Lin, N., De Moel, H., & Michel-Kerjan, E. O. (2014). Evaluating flood resilience strategies for coastal megacities. *Science*, *344*(6183), 473–475. https://doi.org/10.1126/science.1248222

Aerts, J. C. J. H. (2018). A review of cost estimates for flood adaptation. *Water*, *10*(11), 1646. https://doi.org/10.3390/w10111646

Aerts, J. C. J. H., Bates, P. D., Botzen, W. J. W., Bruijn, J. D., Hall, J. W., Hurk, B. V. D., et al. (2024). Exploring the limits and gaps of flood adaptation. *Nature Water*, *2*(8), 719–728. Article 1985. https://doi.org/10.1038/s44221-024-00274-x

Aerts, J. C. J. H., & Botzen, W. J. (2011). Flood-resilient waterfront development in New York city: A study of flood insurance, building codes, and flood zoning. *Annals of the New York Academy of Sciences*, *1227*, 1–82. https://doi.org/10.1111/j.1749-6632.2011.06074.x

Agarwal, D. S., Bharat, A., Kjeldsen, T. R., & Adeyeye, K. (2024). Assessing impact of nature based solutions on peak flow using HEC-HMS. *Water Resources Management*, *38*(3), 1125–1140. https://doi.org/10.1007/s11269-023-03712-9

Andreadis, K. M., Schumann, G. J. P., & Pavelsky, T. (2013). A simple global river bankfull width and depth database. *Water Resources Research*, *49*(10), 7164–7168. https://doi.org/10.1002/wrcr.20440

Archer, N. A., Otten, W., Schmidt, S., Bengough, A. G., Shah, N., & Bonell, M. (2016). Rainfall infiltration and soil hydrological characteristics below ancient forest, planted forest and grassland in a temperate northern climate. *Ecohydrology*, *9*(4), 585–600. https://doi.org/10.1002/eco.1658

Arnell, N. W., & Gosling, S. N. (2016). The impacts of climate change on river flood risk at the global scale. *Climatic Change*, *134*(3), 387–401. https://doi.org/10.1007/s10584-014-1084-5

Bandyopadhyay, S., Jaiswal, R. K., Hegde, V. S., & Jayaraman, V. (2009). Assessment of land suitability potentials for agriculture using a remote sensing and GIS based approach. *International Journal of Remote Sensing*, *30*(4), 879–895. https://doi.org/10.1080/01431160802395235

Barrington-Leigh, C., & Millard-Ball, A. (2017). The world's user-generated road map is more than 80% complete. *PLoS One*, *12*(8), e0180698. https://doi.org/10.1371/journal.pone.0180698

Bernhofen, M. V., Whyman, C., Trigg, M. A., Sleigh, P. A., Smith, A. M., Sampson, C. C., et al. (2018). A first collective validation of global fluvial flood models for major floods in Nigeria and Mozambique. *Environmental Research Letters*, *13*(10), 1–11. Article 104007. https://doi.org/10.1088/1748-9326/aae014

Besnard, S., Koirala, S., Santoro, M., Weber, U., Nelson, J., Gütter, J., et al. (2021). Mapping global forest age from forest inventories, biomass and climate data. *Earth System Science Data*, *13*(10), 4881–4896. https://doi.org/10.5194/essd-13-4881-2021

Brakensiek, D. L., Rawls, W. J., & Stephenson, G. R. (1984). Modifying scs hydrologic soil groups and curve numbers for range land soils, ASAE Paper no. PNR-84-203, St. Joseph, Michigan, USA.

Bril, V., de Bruijn, J., Sadana, T., & Busker, T. (2025). Assessing the effectiveness of nature-based solutions and building-level flood risk reduction measures (1.0) [Dataset]. *Zenodo*. https://doi.org/10.5281/zenodo.15488420

Bubeck, P., De Moel, H., Bouwer, L. M., & Aerts, J. C. J. H. (2011). How reliable are projections of future flood damage? *Natural Hazards and Earth System Sciences*, *11*(12), 3293–3306. https://doi.org/10.5194/nhess-11-3293-2011

Bubeck, P., Dillenardt, L., Alfieri, L., Feyen, L., Thieken, A. H., & Kellermann, P. (2019). Global warming to increase flood risk on European railways. *Climatic Change*, *155*(1), 19–36. https://doi.org/10.1007/s10584-019-02434-5

Burek, P., Satoh, Y., Kahil, T., Tang, T., Greve, P., Smilovic, M., et al. (2019). Development of the community Water Model (CWatM v1. 04) A high-resolution hydrological model for global and regional assessment of integrated water resources management. *Geoscientific Model Development Discussions*, *2019*(7), 1–49. https://doi.org/10.5194/gmd-13-3267-2020

Chan, F. K. S., Yang, L. E., Mitchell, G., Wright, N., Guan, M., Lu, X., et al. (2022). Comparison of sustainable flood risk management by four countries – The United Kingdom, the Netherlands, the United States, and Japan – And the implications for Asian coastal megacities. *Natural Hazards and Earth System Sciences*, *22*(8), 2567–2588. https://doi.org/10.5194/nhess-22-2567-2022

Cooper, M. M., Patil, S. D., Nisbet, T. R., Thomas, H., Smith, A. R., & McDonald, M. A. (2021). Role of forested land for natural flood management in the UK: A review. *Wiley Interdisciplinary Reviews. Water*, *8*(5), e1541. https://doi.org/10.1002/wat2.1541

De Bruijn, J. A., Smilovic, M., Burek, P., Guillaumot, L., Wada, Y., & Aerts, J. C. (2023). GEB v0. 1: A large-scale agent-based socio-hydrological model–simulating 10 million individual farming households in a fully distributed hydrological model. *Geoscientific Model Development*, *16*(9), 2437–2454. https://doi.org/10.5194/gmd-16-2437-2023

De Bruijn, K., Wagenaar, D., Slager, K., De Bel, M., & Burzel, A. (2015). *Updated and improved method for flood damage assessment: SSM2015 (version 2)*. Deltares.

De Jong, J. S., & Asselman, N. (2022). Analyse overstromingen Geulmonding: Watersysteemevaluatie Waterschap Limburg. Retrieved from https://www.deltares.nl/expertise/publicaties/analyse-overstromingen-geulmonding-watersysteemevaluatie-waterschap-limburg

Della Justina, C. R. V., Junior, J. L., Ferreira, M. I. P., & Rodrigues, P. P. G. W. (2019). Nature based solutions as a promising alternative for river restoration and flood reduction. *Boletim do Observatório Ambiental Alberto Ribeiro Lamego*, *13*(2), 198–212. https://doi.org/10.19180/2177-4560.v13n22019p198-212

Deltares. (2024a). Deltares. Retrieved from https://github.com/Deltares/hydromt_sfincs/blob/main/hydromt_sfincs/data/lulc/esa_worldcover_mapping.csv

Deltares. (2024b). SFINCS documentation. Retrieved from https://sfincs.readthedocs.io/en/latest/

De Moel, H., Aerts, J. C., & Koomen, E. (2011). Development of flood exposure in the Netherlands during the 20th and 21st century. *Global Environmental Change*, *21*(2), 620–627. https://doi.org/10.1016/j.gloenvcha.2010.12.005

De Moel, H., & Aerts, J. C. J. H. (2011). Effect of uncertainty in land use, damage models and inundation depth on flood damage estimates. *Natural Hazards*, *58*(1), 407–425. https://doi.org/10.1007/s11069-010-9675-6

De Moel, H., Endendijk, T., Van Ederen, D., Juch, S., & Van Ginkel, K. (2025). *Berekenen van overstromingsschade aan woningen: Nieuwe inzichten voor financiële toepassingen (Report No. 11211522-004-ZWS-0001)*. Deltares. Retrieved from https://publications.deltares.nl/11211522_004_0001.pdf

De Moel, H., van Vliet, M., & Aerts, J. C. (2014). Evaluating the effect of flood damage-reducing measures: A case study of the unembanked area of Rotterdam, the Netherlands. *Regional Environmental Change*, *14*, 895–908. https://doi.org/10.1007/s10113-013-0420-z

de Ruig, L. T., Barnard, P. L., Botzen, W. W., Grifman, P., Hart, J. F., de Moel, H., et al. (2019). An economic evaluation of adaptation pathways in coastal mega cities: An illustration for Los Angeles. *Science of the Total Environment*, *678*, 647–659. https://doi.org/10.1016/j.scitotenv.2019.04.308

Dixon, S. J., Sear, D. A., Odoni, N. A., Sykes, T., & Lane, S. N. (2016). The effects of river restoration on catchment scale flood risk and flood hydrology. *Earth Surface Processes and Landforms*, *41*(7), 997–1008. https://doi.org/10.1002/esp.3919

Eilander, D., Boisgontier, H., Bouaziz, L. J. E., Buitink, J., Couasnon, A., Dalmijn, B., et al. (2025). HydroMT: Automated and reproducible model building and analysis (v1.3.0-rc5) [software]. *Zenodo*. https://doi.org/10.5281/zenodo.17579310

Eilander, D., de Goede, R., Leijnse, T., van Ormondt, M., Nederhoff, K., & Winsemius, H. C. (2025). HydroMT-SFINCS (v1.2.0) [software]. *Zenodo*. https://doi.org/10.5281/zenodo.15270197

Endendijk, T., Botzen, W., de Moel, H., Aerts, J., Duijndam, S., Slager, K., et al. (2023b). Experience from the 2021 floods in the Netherlands: Household Survey results on impacts and responses. *Journal of Coastal and Riverine Flood Risk*, *2*, 9. https://doi.org/10.59490/jcrfr.2023.0009

Endendijk, T., Botzen, W. J. W., De Moel, H., Aerts, J. C. J. H., Slager, K., & Kok, M. (2023a). Flood Vulnerability models and household flood damage Mitigation measures: An econometric analysis of survey data. *Water Resources Research*, *59*(8), e2022WR034192. https://doi.org/10.1029/2022wr034192

ENW (Expertise Netwerk Waterveiligheid) - Task Force Fact Finding Hoogwater. (2021). Hoogwater 2021: Feiten en duiding. Report Version 2 (in Dutch, summary in English). Retrieved from https://www.enwinfo.nl/publish/pages/183541/211102_enw_hoogwater_2021-dv-def.pdf

European Commission. (2021). *Economic appraisal vademecum 2021–2027: General principles and sector applications*. Directorate-General for Regional and Urban Policy.

Ferreira, C. S., Mourato, S., Kasanin-Grubin, M., Ferreira, A. J., Destouni, G., & Kalantari, Z. (2020). Effectiveness of nature-based solutions in mitigating flood hazard in a mediterranean peri-urban catchment. *Water*, *12*(10), 2893. https://doi.org/10.3390/w12102893

Figueiredo, R., Romao, X., & Paupério, E. (2020). Flood risk assessment of cultural heritage at large spatial scales: Framework and application to mainland Portugal. *Journal of Cultural Heritage*, *43*, 163–174. https://doi.org/10.1016/j.culher.2019.11.007

Garcia Alvarez, G., Botzen, W. J. W., Tesselaar, M., Aerts, J. C. J. H., Staccione, A., Mysiak, J., & Bockarjova, M. (2025). The economic benefits of nature-based solution for climate risk: A meta-analysis. *Land Economics*, *101*, 4. https://doi.org/10.3368/le.102.2.110824-0105R1

Guido, B. I., Popescu, I., Samadi, V., & Bhattacharya, B. (2023). An integrated modelling approach to evaluate the impacts of nature-based solutions of flood mitigation across a small watershed in the southeast United States. *Natural Hazards and Earth System Sciences*, *2023*, 1–30. https://doi.org/10.5194/nhess-23-2663-2023

Gutman, J. (2019). Commentary: Urban wetlands restoration as nbs for flood risk mitigation: From positive case to legitimate practice, in the view of evidence-based flood risk policy making. *Nature-Based Flood Risk Management on Private Land: Disciplinary Perspectives on a Multi-disciplinary Challenge*, 127–134. https://doi.org/10.1007/978-3-030-23842-1_13

Herfort, B., Lautenbach, S., De Albuquerque, J. P., Anderson, J., & Zipf, A. (2023). A spatio-temporal analysis investigating completeness and inequalities of global urban building data in OpenStreetMap. *Nature Communications*, *14*(1), 3985. https://doi.org/10.1038/s41467-023-39698-6

Huizinga, J., De Moel, H., & Szewczyk, W. (2017). *Global flood depth-damage functions: Methodology and the database with guidelines, EUR 28552 EN*. Publications Office of the European Union. https://doi.org/10.2760/16510.JRC105688.

Jonkman, S., De Moel, H., Moll, J. R., & Slager, K. (2023). Editorial for the special issue on "2021 Summer Floods in Europe". *Journal of Coastal and Riverine Flood Risk*, *2*. https://doi.org/10.59490/jcrfr.2023.0011

Kadaster. (2025). Kwartaalbericht agrarische grondmarkt 2025-1. Retrieved from https://www.kadaster.nl/-/kwartaalbericht-agrarische-grondmarkt-2025-1

Kalthof, M. W., De Bruijn, J., De Moel, H., Kreibich, H., & Aerts, J. C. (2025). Adaptive behavior of farmers under consecutive droughts results in more vulnerable farmers: A large-scale agent-based modeling analysis in the Bhima basin, India. *Natural Hazards and Earth System Sciences*, *25*(3), 1013–1035. https://doi.org/10.5194/nhess-25-1013-2025

Keesstra, S., Nunes, J., Novara, A., Finger, D., Avelar, D., Kalantari, Z., & Cerdà, A. (2018). The superior effect of nature based solutions in land management for enhancing ecosystem services. *Science of the Total Environment*, *610*, 997–1009. https://doi.org/10.1016/j.scitotenv.2017.08.077

Kellermann, P., Schöbel, A., Kundela, G., & Thieken, A. H. (2015). Estimating flood damage to railway infrastructure–the case study of the March River flood in 2006 at the Austrian Northern Railway. *Natural Hazards and Earth System Sciences*, *15*(11), 2485–2496. https://doi.org/10.5194/nhess-15-2485-2015

Klaassen, W., Bosveld, F., & De Water, E. (1998). Water storage and evaporation as constituents of rainfall interception. *Journal of Hydrology*, *212*, 36–50. https://doi.org/10.1016/S0022-1694(98)00200-5

Kok, M., Slager, K., de Moel, H., Botzen, W., de Bruijn, K., Wagenaar, D., & van Ginkel, K. (2023). Rapid damage assessment caused by the flooding event 2021 in Limburg, Netherlands. *Journal of Coastal and Riverine Flood Risk*, *2*. https://doi.org/10.59490/jcrfr.2023.0010

Koks, E., Rozenberg, J., Zorn, C., Tariverdi, M., Vousdoukas, M., Fraser, S., et al. (2019). A global multi-hazard risk analysis of road and railway infrastructure assets. *Nature Communications*, *10*(1), 2677. https://doi.org/10.1038/s41467-019-10442-3

Kumar, P., Debele, S., Sahani, J., Rawat, N., Martí-Cardona, B., Alfieri, S. M., et al. (2021). Nature-based solutions efficiency evaluation against natural hazards: Modelling methods, advantages and limitations. *Science of the Total Environment*, *784*, 147058. https://doi.org/10.1016/j.scitotenv.2021.147058

Lallemant, D., Hamel, P., Balbi, M., Lim, T. N., Schmitt, R., & Win, S. (2021). Nature-based solutions for flood risk reduction: A probabilistic modeling framework. *One Earth*, *4*(9), 1310–1321. https://doi.org/10.1016/j.oneear.2021.08.010

Le Coent, P., Graveline, N., Altamirano, M. A., Arfaoui, N., Benitez-Avila, C., Biffin, T., et al. (2021). Is-it worth investing in NBS aiming at reducing water risks? Insights from the economic assessment of three European case studies. *Nature-Based Solutions*, *1*, 100002. https://doi.org/10.1016/j.nbsj.2021.100002

Leijnse, T., van Ormondt, M., Nederhoff, K., & van Dongeren, A. (2021). Modeling compound flooding in coastal systems using a computationally efficient reduced-physics solver: Including fluvial, pluvial, tidal, wind-and wave-driven processes. *Coastal Engineering*, *163*, 103796. https://doi.org/10.1016/j.coastaleng.2020.103796

Link, T. E., Unsworth, M., & Marks, D. (2004). The dynamics of rainfall interception by a seasonal temperate rainforest. *Agricultural and Forest Meteorology*, *124*(3–4), 171–191. https://doi.org/10.1016/j.agrformet.2004.01.010

Martin, J. G., Scolobig, A., Linnerooth-Bayer, J., Irshaid, J., Rodriguez, J. J. A., Fresolone-Caparrós, A., & Oen, A. (2025). The nature-based solution implementation gap: A review of nature-based solution governance barriers and enablers. *Journal of Environmental Management*, *388*, 126007. https://doi.org/10.1016/j.jenvman.2025.126007

Merz, B., & Thieken, A. H. (2009). Flood risk curves and uncertainty bounds. *Natural Hazards*, *51*(3), 437–458. https://doi.org/10.1007/s11069-009-9452-6

Mester, B., Willner, S. N., Frieler, K., & Schewe, J. (2021). Evaluation of river flood extent simulated with multiple global hydrological models and climate forcings. *Environmental Research Letters*, *16*(9), 094010. https://doi.org/10.1088/1748-9326/ac188d

Mohr, S., Ehret, U., Kunz, M., Ludwig, P., Caldas-Alvarez, A., Daniell, J. E., et al. (2023). A multi-disciplinary analysis of the exceptional flood event of July 2021 in central Europe. Part 1: Event description and analysis. *Natural Hazards and Earth System Sciences Discussions*, *2022*(2), 1–44. https://doi.org/10.5194/nhess-23-525-2023

Moos, C., Bebi, P., Schwarz, M., Stoffel, M., Sudmeier-Rieux, K., & Dorren, L. (2018). Ecosystem-based disaster risk reduction in mountains. *Earth-Science Reviews*, *177*, 497–513. https://doi.org/10.1016/j.earscirev.2017.12.011

Mortensen, E., Tiggeloven, T., Haer, T., Van Bemmel, B., Le Bars, D., Muis, S., et al. (2024). The potential of global coastal flood risk reduction using various DRR measures. *Natural Hazards and Earth System Sciences*, *24*(4), 1381–1400. https://doi.org/10.5194/nhess-24-1381-2024

Mubeen, A., Ruangpan, L., Vojinovic, Z., Sanchez Torrez, A., & Plavšić, J. (2021). Planning and suitability assessment of large-scale nature-based solutions for flood-risk reduction. *Water Resources Management*, *35*(10), 3063–3081. https://doi.org/10.1007/s11269-021-02848-w

Munich, R. E. (2023). Flood risks on the rise – Greater loss prevention is needed. https://www.munichre.com/en/risks/natural-disasters/floods.html

Muñoz Sabater, J. (2019). ERA5-Land hourly data from 1950 to present. *Copernicus Climate Change Service (C3S) Climate Data Store (CDS)*. https://doi.org/10.24381/cds.e2161bac

Nadal-Romero, E., Llena, M., Melani Cortijos-López, M., & Lasanta, T. (2023). Afforestation after land abandonment as a nature based solution in mediterranean mid-mountain areas: Implications and research gaps. *Current Opinion in Environmental Science & Health*, *34*, 100481. https://doi.org/10.1016/j.coesh.2023.100481

Nicolai, N., van der Vliet, N., & Lugt, D. (2024). *Neerslagstatistiek KNMI' 23 (Report No. 2024-37)*. Stichting Toegepast Onderzoek Waterbeheer. Retrieved from https://www.stowa.nl/sites/default/files/assets/PUBLICATIES/Publicaties%202024/STOWA_2024-37-totstandkoming-neerslagproducten-knmi2023.pdf

Nirandjan, S., Koks, E. E., Ye, M., Pant, R., Van Ginkel, K. C., Aerts, J. C., & Ward, P. J. (2024). Physical vulnerability database for critical infrastructure hazard risk assessments–a systematic review and data collection. *Natural Hazards and Earth System Sciences*, *24*(12), 4341–4368. https://doi.org/10.5194/nhess-24-4341-2024

Nisbet, T. R. (2005). *Water use by trees. Information note of forest research*. Forestry Commission.

Oostwegel, L. J., Evaz Zadeh, T., Lingner, L., & Schorlemmer, D. (2023). A global and dynamic completeness assessment of the OpenStreetMap buildings. *Proceedings of the OSM Science*, 6–9. https://doi.org/10.5281/zenodo.10443307

Opperman, J. J., & Galloway, G. E. (2022). Nature-based solutions for managing rising flood risk and delivering multiple benefits. *One Earth*, *5*(5), 461–465. https://doi.org/10.1016/j.oneear.2022.04.012

Otto, A., Hornberg, A., & Thieken, A. H. (2016). Local controversies of flood risk reduction measures in Germany. An explorative overview and recent insights. *Journal of Flood Risk Management*, *11*(S1), S382–S394. https://doi.org/10.1111/jfr3.12227

Parodi, M. U., Giardino, A., Van Dongeren, A., Pearson, S. G., Bricker, J. D., & Reniers, A. J. (2020). Uncertainties in coastal flood risk assessments in small island developing states. *Natural Hazards and Earth System Sciences*, *20*(9), 2397–2414. https://doi.org/10.5194/nhess-20-2397-2020

Poggio, L., de Sousa, L. M., Batjes, N. H., Heuvelink, G. B. M., Kempen, B., Ribeiro, E., & Rossiter, D. (2021a). SoilGrids 2.0: Producing soil information for the globe with quantified spatial uncertainty. *SOIL*, *7*(1), 217–240. https://doi.org/10.5194/soil-7-217-2021

Poggio, L., de Sousa, L. M., Batjes, N. H., Heuvelink, G. B. M., Kempen, B., Ribeiro, E., & Rossiter, D. (2021b). SoilGrids 2.0 [Dataset]. https://files.isric.org/soilgrids/latest/

Provincie Limburg. (2022). Limburgse aanpak bossen. Retrieved from https://www.limburg.nl/publish/pages/4507/2212_8223_limburgse_aanpak_bossen.pdf

Pudar, R., Plavšić, J., & Todorović, A. (2020). Evaluation of green and grey flood mitigation measures in rural watersheds. *Applied Sciences*, *10*(19), 6913. https://doi.org/10.3390/app10196913

Röbke, B. R., Leijnse, T., Winter, G., van Ormondt, M., van Nieuwkoop, J., & de Graaff, R. (2021). Rapid assessment of tsunami offshore propagation and inundation with D-FLOW flexible mesh and SFINCS for the 2011 Tōhoku tsunami in Japan. *Journal of Marine Science and Engineering*, *9*(5), 453. https://doi.org/10.3390/jmse9050453

Ruangpan, L., Vojinovic, Z., Di Sabatino, S., Leo, L. S., Capobianco, V., Oen, A. M., et al. (2020). Nature-based solutions for hydro-meteorological risk reduction: A state-of-the-art review of the research area. *Natural Hazards and Earth System Sciences*, *20*(1), 243–270. https://doi.org/10.5194/nhess-20-243-2020

Ruangpan, L., Vojinovic, Z., Plavšić, J., Curran, A., Rosic, N., Pudar, R., et al. (2024). Economic assessment of nature-based solutions to reduce flood risk and enhance co-benefits. *Journal of Environmental Management*, *352*, 119985. https://doi.org/10.1016/j.jenvman.2023.119985

Rüegg, J., Moos, C., Gentile, A., Luisier, G., Elsig, A., Prasicek, G., & Otero, I. (2022). An approach to evaluate mountain forest protection and management as a means for flood mitigation. *Frontiers in Forests and Global Change*, *5*, 785740. https://doi.org/10.3389/ffgc.2022.785740

Sampson, C. C., Smith, A. M., Bates, P. D., Neal, J. C., Alfieri, L., & Freer, J. E. (2015). A high-resolution global flood hazard model. *Water Resources Research*, *51*(9), 7358–7381. https://doi.org/10.1002/2015WR016954

Santoro, S., Pluchinotta, I., Pagano, A., Pengal, P., Cokan, B., & Giordano, R. (2019). Assessing stakeholders' risk perception to promote Nature Based Solutions as flood protection strategies: The case of the Glinščica river (Slovenia). *Science of the Total Environment*, *655*, 188–201. https://doi.org/10.1016/j.scitotenv.2018.11.116

Sebastian, A., Bader, D. J., Nederhoff, C. M., Leijnse, T. W. B., Bricker, J. D., & Aarninkhof, S. G. J. (2021). Hindcast of pluvial, fluvial, and coastal flood damage in Houston, Texas during Hurricane Harvey (2017) using SFINCS. *Natural Hazards*, *109*(3), 2343–2362. https://doi.org/10.1007/s11069-021-04922-3

Sieg, T., Schinko, T., Vogel, K., Mechler, R., Merz, B., & Kreibich, H. (2019). Integrated assessment of short-term direct and indirect economic flood impacts including uncertainty quantification. *PLoS One*, *14*(4), e0212932. https://doi.org/10.1371/journal.pone.0212932

Sieg, T., & Thieken, A. H. (2022). Improving flood impact estimations. *Environmental Research Letters*, *17*(6), 064007. https://doi.org/10.1088/1748-9326/ac6d6c

Slager, K., de Moel, H., & de Jong, J. (2021). Maximum flood extents Limburg floods July 2021 (Version 1) [Dataset]. *4TU.ResearchData*. https://doi.org/10.4121/16817389.V1

Slager, K., & Wagenaar, D. (2017). Standaardmethode 2017: Schade en slachtoffers als gevolg van overstromingen.

Strock, J. S., Johnson, J. M., Tollefson, D., & Ranaivoson, A. (2022). Rapid change in soil properties after converting grasslands to crop production. *Agronomy Journal*, *114*(3), 1642–1654. https://doi.org/10.1002/agj2.21045

Teng, J., Jakeman, A. J., Vaze, J., Croke, B. F., Dutta, D., & Kim, S. J. E. M. (2017). Flood inundation modelling: A review of methods, recent advances and uncertainty analysis. *Environmental Modelling & Software*, *90*, 201–216. https://doi.org/10.1016/j.envsoft.2017.01.006

Tóth, B., Weynants, M., Nemes, A., Makó, A., Bilas, G., & Tóth, G. (2015). New generation of hydraulic pedotransfer functions for Europe. *European Journal of Soil Science*, *66*(1), 226–238. https://doi.org/10.1111/ejss.12192

Tsiokanos, A., Rutten, M., Van Der Ent, R. J., & Uijlenhoet, R. (2024). Flood drivers and trends: A case study of the Geul River catchment (the Netherlands) over the past half century. *Hydrology and Earth System Sciences*, *28*(14), 3327–3345. https://doi.org/10.5194/hess-28-3327-2024

Turkelboom, F., Demeyer, R., Vranken, L., De Becker, P., Raymaekers, F., & De Smet, L. (2021). How does a nature-based solution for flood control compare to a technical solution? Case study evidence from Belgium. *Ambio*, *50*(8), 1431–1445. https://doi.org/10.1007/s13280-021-01548-4

Vangelis, H., Zotou, I., Kourtis, I. M., Bellos, V., & Tsihrintzis, V. A. (2022). Relationship of rainfall and flood return periods through hydrologic and hydraulic modeling. *Water*, *14*(22), 3618. https://doi.org/10.3390/w14223618

Van Ginkel, K., Dottori, F., Alfieri, L., Feyen, L., & Koks, E. (2021). Flood risk assessment of the European road network. *Natural Hazards and Earth System Sciences*, *21*(3), 1011–1027. https://doi.org/10.5194/nhess-21-1011-2021

Van Heeringen, K., Asselman, N., Overeem, A., Beersma, J., & Philip, S. (2022). Analyse overstroming Valkenburg: Watersysteemevaluatie Waterschap Limburg. (in Dutch) https://publications.deltares.nl/11207700_000_0014.pdf

van Ormondt, M., Leijnse, T., Nederhoff, K., de Goede, R., van Dongeren, A., Bovenschen, T., & van Asselt, K. (2025). SFINCS: Super-fast INundation of CoastS model (2.2.0 col d'Eze Release 2025.01) [software]. *Zenodo*. https://doi.org/10.5281/zenodo.13691724

Viglione, A., & Blöschl, G. (2009). On the role of storm duration in the mapping of rainfall to flood return periods. *Hydrology and Earth System Sciences*, *13*(2), 205–216. https://doi.org/10.5194/hess-13-205-2009

Vikolainen, V., Bressers, H., & Lulofs, K. (2013). The role of Natura 2000 and project design in implementing flood defence projects in the Scheldt estuary. *Journal of Environmental Planning and Management*, *56*(9), 1359–1379. https://doi.org/10.1080/09640568.2012.724014

Vojinovic, Z., Alves, A., Gómez, J. P., Weesakul, S., Keerakamolchai, W., Meesuk, V., & Sanchez, A. (2021). Effectiveness of small-and large-scale Nature-Based Solutions for flood mitigation: The case of Ayutthaya, Thailand. *Science of The Total Environment*, *789*, 147725. https://doi.org/10.1016/j.scitotenv.2021.147725

Waterboard Limburg. (2019a). Locations of waterbuffers. Retrieved on 15-01-2025 from Retrieved from https://ws-limburg.maps.arcgis.com/apps/webappviewer/index.html?id=491934138032419e9d2aed49b12fe5c3

Wing, O. E., Bates, P. D., Sampson, C. C., Smith, A. M., Johnson, K. A., & Erickson, T. A. (2017). Validation of a 30 m resolution flood hazard model of the conterminous United States. *Water Resources Research*, *53*(9), 7968–7986. https://doi.org/10.1002/2017WR020917

Wu, G. L., Liu, Y., Fang, N. F., Deng, L., & Shi, Z. H. (2016). Soil physical properties response to grassland conversion from cropland on the semi-arid area. *Ecohydrology*, *9*(8), 1471–1479. https://doi.org/10.1002/eco.1740

Zanaga, D., Van De Kerchove, R., Daems, D., De Keersmaecker, W., Brockmann, C., Kirches, G., et al. (2022). ESA WorldCover 10 m 2021 v200 [Dataset]. *WorldCover 10 m 2021 v200*. https://doi.org/10.5281/zenodo.7254221

Zeleňáková, M., Gaňová, L., & Diaconu, D. C. (2020). *Flood damage assessment and management, water science and technology Library* (Vol. 94, pp. 41–91). Springer. https://doi.org/10.1007/978-3-030-50053-5_2

Zema, D. A., Plaza-Alvarez, P. A., Xu, X., Carra, B. G., & Lucas-Borja, M. E. (2021). Influence of forest stand age on soil water repellency and hydraulic conductivity in the Mediterranean environment. *Science of the Total Environment*, *753*, 142006. https://doi.org/10.1016/j.scitotenv.2020.142006

References From the Supporting Information

Fan, N., Wang, Y., Yang, X., Li, J., Kang, J., Liu, Q., & Zhang, Z. (2024). Suitability assessment for forest landscape restoration based on species diversity conservation. *Frontiers in Forests and Global Change*, *7*, 1252077. https://doi.org/10.3389/ffgc.2024.1252077

Municipality Vught. (2023). Bijlage 1.1 Landschappelijk inpassingsplan. Retrieved from https://vught.bestuurlijkeinformatie.nl/Agenda/Document/23de3210-3562-483b-94a5-2323ca9f9b05?documentId=1fe7ed85-aa7a-4e3d-a487-c66ff6134317&agendaItemId=65a509b2-486c-4bd7-a67e-c65df79f3585

N&L. (2024). Standkaartkostprijs directe werkzaamheden natuur-en landschapsbeheer. Retrieved from https://www.bij12.nl/wp-content/uploads/2024/08/Standaardkostprijzen-Natuur-en-Landschap-2024-beheerjaar-2025.pdf

Teeuwen, S., Reichgelt, A., & Oldenburger, J. (2020). Factsheets – Kostenindicatie aanleg nieuw bos en landschapselementen. Retrieved from https://gereedschapskistbosennatuur.nl/wp-content/uploads/2024/11/factsheets-kostenindicatie-aanleg-bos-landschapselementen-2020.pdf

Waterboard Limburg. (2019b). Koersvast op weg naar een nieuw decennium – Voorjaarsrapportage 2019. Retrieved from https://www.waterschaplimburg.nl/publish/pages/4385/voorjaarsrapportage_2019_1.pdf

Waterboard Limburg. (2020). Jaarrekening/jaarverslag 2020. Retrieved from https://www.waterschaplimburg.nl/publish/pages/4854/jaarrekening_jaarverslag_2020.pdf

Waterboard Limburg. (2025). Algemene informatie stimuleringsregeling water vasthouden 2025. Retrieved from https://www.waterschaplimburg.nl/vooragrariers/stimuleringsregeling-water-vasthouden/algemene-informatie/